Time dependent impact of copper oxide nanomaterials on the expression of genes associated with oxidative stress, metal binding, inflammation and mucus secretion in single and co-culture intestinal in vitro models

Toxicology in Vitro 74 (2021) 105161

Contents lists available at ScienceDirect

Toxicology in Vitro

journal homepage: www.elsevier.com/locate/toxinvit

Time dependent impact of copper oxide nanomaterials on the expression of genes associated with oxidative stress, metal binding, inflammation and mucus secretion in single and co-culture intestinal *in vitro* models

Victor C. Ude *, David M. Brown, Vicki Stone, Helinor J. Johnston *

Nano Safety Research Group, School of Engineering and Physical Sciences, Institute of Biological Chemistry, Biophysics and Bioengineering, Heriot-Watt University, Edinburgh EH14 4AS, UK

ARTICLE INFO

Editor: Martin Leonard

Keywords:
Copper oxide nanomaterials
Intestine
Haem oxygenase
Mucin 2
Metallothionein
Interleukin 8

ABSTRACT

The potential for ingestion of copper oxide nanomaterials (CuO NMs) is increasing due to their increased exploitation. Investigation of changes in gene expression allows toxicity to be detected at an early stage of NM exposure and can enable investigation of the mechanism of toxicity. Here, undifferentiated Caco-2 cells, differentiated Caco-2 cells, Caco-2/HT29-MTX (mucus secreting) and Caco-2/Raji B (M cell model) co-cultures were exposed to CuO NMs and copper sulphate ($CuSO_4$) in order to determine their impacts. Cellular responses were measured in terms of production of reactive oxygen species (ROS), the gene expression of an antioxidant (haem oxygenase 1 (*HMOX1*)), the pro-inflammatory cytokine (interleukin 8 (*IL8*)), the metal binding (metallothionein 1A and 2A (*MT1A* and *MT2A*)) and the mucus secreting (mucin 2 (*MUC2*)), as well as HMOX-1 protein level. While $CuSO_4$ induced ROS production in cells, no such effect was observed for CuO NMs. However, these particles did induce an increase in the level of HMOX-1 protein and upregulation of *HMOX1*, *MT2A*, *IL8* and *MUC2* genes in all cell models. In conclusion, the expression of *HMOX1*, *IL8* and MT2A were responsive to CuO NMs at 4 to 12 h post exposure when investigating the toxicity of NMs using intestinal *in vitro* models. These findings can inform the selection of endpoints, timepoints and models when investigating NM toxicity to the intestine *in vitro* in the future.

1. Introduction

Intentional and accidental ingestion of nanomaterials (NMs) is likely to rise due to their increased exploitation in a range of products. For example, copper oxide (CuO) NMs are used for ink production, food contact materials, textiles, wood preservation, intrauterine devices and incorporated into heat transfer fluids and semiconductors (Gabbay, 2006; Araújo et al., 2014; Civardi et al., 2015). Accidental ingestion of CuO NMs is likely through leachates from food contact materials, *via* mucociliary clearance of inhaled particles which are then swallowed, and due to hand to mouth exposure (Ude et al., 2017). Several intestinal cell lines such as Caco-2 (human colon colorectal adenocarcinoma), TC-7 (clones isolated from Caco-2 cells), SW620 (human Caucasian colon adenocarcinoma), HT29 and T_{84} (human colon carcinoma) (Pavelić et al., 2001; Bricks et al., 2014) have been used to assess the toxicity of ingested substances. However, Caco-2 cell lines are more frequently used due to their ability to spontaneously differentiate and exhibit an *in vivo*-like intestinal morphology after 21 days of culture (Sambuy et al., 2001; Sambuy et al., 2005). Due to the absence of specific *in vivo* characteristics of the intestine in monocultures of Caco-2 cells, they can also be co-cultured with other cell lines in order to more closely mimic the structure and function of the intestine *in vivo* (Antunes et al., 2013; Schimpel et al., 2014; Georgantzopoulou et al., 2016; Ude et al., 2019a). For example, culturing differentiated Caco-2 with lymphocytes (*e.g.* Raji

Abbreviations: $CuSO_4$, Copper sulphate; CuO NMs, Copper oxide nanomaterials; ROS, Reactive oxygen species; TEER, Transepithelial electrical resistance; ELISA, Enzyme-linked immuno-sorbent assay; CNTs, Carbon nanotubes; HMOX1, Haem oxygenase 1; IL8, Interleukin 8; MT2A, Metallothionein 2A; MT1A, Metallothionein 1A; MUC2, Mucin 2; ANOVA, Analysis of variance; EDTA, Ethylenediaminetetraacetic acid; PBS, Phosphate buffered saline; FBS, Fetal bovine serum; DMEM, 4.5 g/l glucose Dulbecco's modified eagle medium; DCFH-DA, Dichloro-dihyro-fluorescein diacetate; NEAA, Non-essential amino acid; Ct, Threshold cycle; cDNA, Complementary deoxyribonucleic acid; GAPDH, Glyceraldehyde 3-phosphate dehydrogenase; RT-qPCR, Real time quantitative polymerase chain reaction.

* Corresponding author.
E-mail addresses: V.Ude@hw.ac.uk (V.C. Ude), d.brown@hw.ac.uk (D.M. Brown), v.stone@hw.ac.uk (V. Stone), h.johnston@hw.ac.uk (H.J. Johnston).

https://doi.org/10.1016/j.tiv.2021.105161
Received 27 August 2020; Received in revised form 5 March 2021; Accepted 4 April 2021
Available online 9 April 2021

B cells) leads to the development of M cells which are responsible for trafficking antigens, particles and microbial pathogens to the underlying immune system in the intestine (Lefebvre et al., 2015; Jepson and Clark, 2001; Gullberg et al., 2000). In addition, culturing differentiated Caco-2 cells with HT29-MTX cells incorporates mucus secreting cells into the model (Mahler et al., 2009), which is important as mucus has defensive properties and is known to prevent infection and activation of inflammation that can damage the intestine (Hansson, 2012).

It is established that some NMs can exhibit toxicity to different target sites *in vitro* and *in vivo via* the activation of oxidative and inflammatory responses (reviewed by Ivask et al., 2014; Stone et al., 2017, Johnston et al., 2018). Of benefit is that investigation of gene expression when assessing NM toxicity can allow assessment of potential effects at earlier time points (*e.g.* 2–4 h) than other approaches, as well as providing information on their mechanism of action. This study has focused on assessment of genes involved in oxidative stress, inflammation, mucus production and metal binding for reasons outlined below.

During oxidative stress there is an imbalance between the levels of damaging reactive oxygen species (ROS) and protective antioxidants, which favours the production of ROS and depletion of antioxidants (Valko et al., 2007). Oxidative stress is associated with several pathological conditions in the GI tract such as inflammatory bowel disease, gastrointestinal ulcers and various intestinal malignancies (Bhattacharyya et al., 2014; Kim et al., 2014). Production of intracellular ROS is commonly assessed in NM hazard studies as an indicator of their potential to cause toxicity. For example, CuO NMs have been shown to stimulate the greatest increase in ROS production in A549 human lung epithelial cells compared to titanium oxide (TiO_2), zinc oxide (ZnO), $CuZnFe_2O_4$, iron(II,III) oxide (Fe_3O_4) and iron(III) oxide (Fe_2O_3) NMs (Karlsson et al., 2008; Boyles et al., 2016). In parallel to assessing ROS production, it is recommended that the levels/activities of antioxidants are assessed to determine the involvement of oxidative stress in NM toxicity. For gene expression, the levels of haem oxygenase, catalase, superoxide dismutase and glutathione S-transferase have been examined when studying the toxicity of NMs in Caco-2 and A549 cells (Song et al., 2014; Bajak et al., 2015; Sthijns et al., 2017; Abbasi-Oshaghi et al., 2019).

NM mediated oxidant production can stimulate the activation of several signalling pathways leading to a myriad of cellular responses, typically *via* activation of transcription factors (Brown et al., 2004; Brown et al., 2010; Marano et al., 2011; Zhang et al., 2016; Yan et al., 2016). For example, oxidative stress may lead to an inflammatory response *via* activation of the redox sensitive nuclear factor kappa B (NF-κB), which is responsible for controlling the transcription of pro-inflammatory genes such as interleukin-1 beta (*IL-1β*), interleukin-8 (*IL-8*), and tumour necrosis factor-alpha (*TNF-α*) (Huang et al., 2010; Piret et al., 2012a). Inflammatory and oxidative responses therefore commonly occur in concert.

In vitro and *in vivo* studies have shown that NMs can activate inflammatory responses at a range of target sites, including the intestine. For example, CuO NMs have been shown to induce IL-8 protein release by undifferentiated Caco-2 cells, differentiated Caco-2 cells, Caco-2/HT29-MTX and Caco-2/Raji B co-cultures (Piret et al., 2012b; Ude et al., 2017; Ude et al., 2019a). TiO_2, ZnO and silicon oxide (SiO_2) have also demonstrated increased IL-8 release when exposed to undifferentiated and differentiated Caco-2 cells (Gerloff et al., 2013: Krüger et al., 2014; Tada-Oikawa et al., 2016).

Intestinal mucus functions as a first line of defence to invading pathogens. Previous research has focused on the ability of NMs to penetrate the mucus layer and neglected to investigate the impact of NMs on mucus secretion (Mercier-Bonin et al., 2018). Investigation of the impact of NMs on mucus secretion, *via* assessment of changes in the expression of the genes which encode mucus proteins (*e.g. MUC2*) is therefore timely. However, an increase in *MUC2* expression *in vivo*, along with low viscoelastic characteristics and barrier integrity dysfunction after inflammation as a result of bacteria has been reported (*e.g.* Cornick et al., 2015). Also, exposure of intestinal goblet-like cells (LS174T) to acetaldehyde increased expression of *MUC2* which was reported to have a detrimental effect on mucus function (Elamin et al., 2014), suggesting that some cells may increase secretion of less functional mucus when exposed to chemicals.

Metallothioneins (MT) can shield cells against damage caused by metals such as ROS production, DNA damage, oxidative stress, cell damage, angiogenesis, apoptosis, and increase cell proliferation (Takahashi, 2012; Carpene et al., 2007; Ruttkay-Nedecky et al., 2013). Elevated cellular Cu concentrations can trigger the transcription of MT genes and MT protein synthesis in mice (Bremner, 1987; Suzuki et al., 2002). When the level of MT protein is unable to control the increased copper level, the saturated Cu-MT complex may function as a pro-oxidant by Cu ions released from the saturated thiol group (Jiménez et al., 2002; Liu et al., 2001). No studies were identified that investigated MT levels in intestinal cells following exposure to CuO NMs. However, an upregulation of MT expression was observed 24 h post exposure of astrocytes (Luther et al., 2012) and Caco-2 cells (Zhang et al., 2015) to Ag NMs (75 nm).

Previously, different *in vitro* intestinal models (differentiated Caco-2 cells, Caco-2/HT29-MTX and Caco-2/Raji B co-cultures) were demonstrated to respond differently when exposed to CuO NMs and $CuSO_4$, with undifferentiated Caco-2 cells being the most susceptible to toxic effects and the Caco-2/HT29-MTX co-culture being less sensitive (Ude et al., 2017; Ude et al., 2019a). However, when CuO NMs and $CuSO_4$ were compared using the individual intestinal models, they showed similar impacts in terms of IL-8 protein secretion, transepithelial electrical resistance (TEER) measurement, immunostaining of tight junction protein (Zonula ocludin-1) and light microscopy (Ude et al., 2017; Ude et al., 2019a). Differentiated Caco-2 cells, Caco-2/Raji B and Caco-2/HT29-MTX co-cultures have also been used for transport studies to assess NM penetration across the intestinal barrier (Des Rieux et al., 2005; Brun et al., 2014; Akbari et al., 2017; Cabellos et al., 2017; Ude et al., 2019a). Interestingly, De Jong et al. (2019) has demonstrated morphological changes in stomach, liver and bone marrow histopathology, including effects on white blood cells and increased alanine and aspartate transaminases in blood after exposure of rats *via* oral gavage to the CuO NMs used in this study at a dose of 32 mg/kg body weight consecutively for 5 days and euthanised at day 26. However, changes in gene expression in these *in vitro* models following NM exposure has not been investigated previously. Therefore, this study seeks to investigate time and concentration dependent impacts of CuO NMs and $CuSO_4$ to the intestine *in vitro via* investigation of the levels of haem oxygenase (HMOX-1) protein, and expression of selected genes involved in oxidative stress *HMOX1*, inflammation (interleukin 8 (*IL8*)), mucus secretion (mucin 2 (*MUC2*) and metal binding (*MT1A* and *MT2A*) to compare the responsiveness of four intestinal *in vitro* models. The results from this study will help to decipher the mechanism underlying the toxicity of CuO NMs to the intestine and inform the selection of models and endpoints to prioritise when investigating NM toxicity to the intestine *in vitro* in the future. In this study, it was hypothesized that CuO NMs would induce time and concentration dependent upregulation of genes associated with oxidative stress, inflammation, mucus secretion and metal binding and that the level of gene upregulation will be higher in the single cell culture compared to the co-culture models.

2. Materials and methods

2.1. Nanomaterials and characterisation

The CuO NMs used for this study was a gift from project partners in the FP7 funded project Sustainable Nanotechnologies (SUN) and sourced from Plasma Chem, GmbH (Berlin, Germany). The CuO NMs were supplied in a powdered form. The size range of the crystalline CuO NMs as provided by the manufacturer was between 15 and 20 nm. The specific surface area (47 m^2/g) and density (6.3 g/cm^3) as provided in

the data sheet were assessed following Brunauer–Emmett–Teller (BET) method. Further characterisation of the CuO NMs was performed using X-ray diffraction (XRD), Inductive Coupled Plasma Optical Emission Spectrometry (ICP-OES) and Transmission Electron Microscopy (TEM) which were reported previously (Gosens et al., 2016). The dissolution of CuO NMs, hydrodynamic diameter (size) and zeta potential following dispersion in complete medium were also previously investigated using the dynamic light scattering (DLS) method (Ude et al., 2017).

The dispersion of CuO NMs was carried out as described previously (Jacobsen et al., 2010; Ude et al., 2017). Briefly, CuO NMs was dispersed in 2% Fetal bovine serum (FBS) (Gibco Life Technologies) in Milli Q deionised water at a concentration of 1 Cu mg/ml and sonicated with an Ultrawave Sonicator (QS25) and energy density of 400 J/ml for 16 min without pause. After the sonication the samples were diluted in 4.5 g/l glucose Dulbecco's modified eagle medium (DMEM) (Sigma) cell culture medium to the required concentrations and used immediately. $CuSO_4$ was also prepared in the same way as CuO NMs. Previous studies informed the sub-lethal concentration of CuO NMs and $CuSO_4$ selected for this study (Ude et al., 2017). Viability of differentiated cells and co-culture models were assessed after exposure to CuO NMs and $CuSO_4$ in our previous studies *via* nuclei counts and light microscopy (Ude et al., 2017; Ude et al., 2019a), and no loss of cell viability was observed at the concentration selected for this study.

2.2. Cell culture

The human colon colorectal adenocarcinoma Caco-2 cell line (Caco-2 ATCC® HTB-37™) and Human Burkitti's lymphoma; B lymphocyte (Raji B) cell line (Raji ATCC® CCL-86™) were obtained from the American Type Culture Collection (ATCC) (USA). The HT29-MTX clone E-12 cell line was obtained from the European Collection of Authentic Cell Culture (ECACC) (UK) (Behrens et al., 2001). Caco-2 and HT29-MTX cells were maintained in DMEM (Sigma) supplemented with 10% heat inactivated FBS (Gibco Life Technologies), 100 U/ml Penicillin/Streptomycin (Gibco Life Technologies), 100 IU/ml non-essential amino acid (NEAA) (Gibco Life Technologies), and 2 mM L- glutamine (Gibco Life Technologies) (termed DMEM complete cell culture medium), at 37 °C and 5% CO_2 and 95% humidity. Raji B cells were maintained in Roswell Park Memorial Institute (RPMI) 1640 Medium (Gibco Life Technologies) supplemented with 10% heat inactivated FBS (Gibco Life Technologies), 100 U/ml Penicillin/Streptomycin (Gibco Life Technologies) (termed RPMI complete cell culture medium) and at 37 °C, 5% CO_2 and 95% humidity. For all the experiments, Caco-2 and HT29-MTX cells at passage numbers 45 to 50 and Raji B cells at passage numbers 10 to 15 were used.

For undifferentiated cells, 1.56×10^5 cells/cm^2 of Caco-2 cells were seeded into a 24 well plate (Costar Corning, Flintshire, UK) at 37 °C, 5% CO_2 for 24 h.

To obtain differentiated cells, Caco-2 cells were seeded into the apical (AP) compartment of the transwell insert (3.0 μm pore polycarbonate transwell inserts with growth area of 1.12 cm^2 (Costar corning, Flintshire, UK)) in a 12 well plate at a concentration of 3.13×10^5 cells/cm^2 (500 μl/well) in DMEM complete cell culture medium. The basolateral (BL) compartment was filled with 1.5 ml of DMEM complete cell culture medium. The cells were cultured at 37 °C, 5% CO_2 and 95% humidity for 21 days with medium changed every two days for 16 days and then everyday up to the 21st day. TEER measures were taken every 2 days from the 5th day to monitor cell differentiation following the method described in our previous study (Ude et al., 2017).

The Caco-2/Raji B co-culture (M cell model) was cultured following the method described previously (Ude et al., 2019a). Briefly, a concentration of 3.13×10^5 cells/cm^2 of Caco-2 cells (in 0.5 ml DMEM complete cell culture medium) was seeded into the AP compartment of 3.0 μm pore polycarbonate transwell inserts in a 12- well plate and maintained at standard cell culture condition. The AP (0.5 ml) and BL (1.5 ml) medium were changed every 2 days. Raji B cells were seeded at a concentration of 5×10^5 cells/ml (in 1.5 ml DMEM complete cell culture medium) into the BL compartment on day 15. The co-culture was cultured for 5 days and medium changed every day at the AP compartment. TEER measures were taken every 2 days starting from the 5 day to monitor cell differentiation.

The Caco-2/HT29-MTX (mucus secreting) co-culture model was cultured following the method described previously (Ude et al., 2019a). Briefly, a concentration of 3.13×10^5 cells/cm^2 of Caco-2 and HT29-MTX cells at a ratio of 9:1 was seeded into the AP compartment of 3.0 μm pore polycarbonate transwell inserts in a 12-well plate (Costar corning, Flintshire, UK). The cells were incubated in standard cell culture condition for 20–21 days and the medium changed every 2 days for the first 16 days followed by every day up to the 21st day. TEER measures were taken every 2 days to monitor cell differentiation from the fifth day.

The intestinal cell models (differentiated Caco-2 cells, Caco-2/Raji B and Caco-2/HT29-MTX co-cultures) were checked for differentiation status *via* measurement of TEER, alcian blue staining (for mucus production), Wheat Germ Agglutinin (WGA) staining (to identify M cells), ZO-1 staining (to assess the formation of tight junctions) and visualisation of microvilli using Scanning Electron Microscopy (SEM) as described previously (Ude et al., 2017; Ude et al., 2019a). Differentiated Caco-2 cells, Caco-2/HT29-MTX and Caco-2/Raji B co-culture with TEER values of greater than 500 Ω.cm^2 were used for this study.

2.3. Evaluation of cell free ROS production

Cell free ROS production by CuO NMs and $CuSO_4$ was evaluated using the dichloro-dihyro-fluorescein diacetate (DCFH-DA) assay, following the method described previously (Foucaud et al., 2007; Sauvain et al., 2013; Ude et al., 2019b). Briefly, 1 mM DCFH-DA (in methanol) was prepared then diluted to a concentration of 0.2 mM in 0.01 M NaOH to hydrolyse the probe and left at room temperature for 30 min in the dark. Next, 0.1 M PBS (pH 7.4) was added to stop the reaction, giving a concentration of 0.05 mM DCF (termed the reaction mix). The solution was placed on ice and used immediately. In addition, equivalent volumes of 0.01 M NaOH, 0.1 M PBS solution (pH 7.4) and methanol without DCFH-DA was prepared.

The reaction mix or the mixture without DCFH-DA was transferred to the wells of a black clear bottom 96 well plate (225 μl/well) in triplicate. Thereafter, 25 μl of MEM complete cell culture medium without phenol red (negative control), 1 mM/cm^2 H_2O_2 or 3.17, 6.34 or 12.68 Cu μg/cm^2 of CuO NMs or $CuSO_4$ (in MEM complete cell culture medium without phenol red) were added in triplicate. Using a SpectraMax M5 microplate reader (California USA), fluorescence was measured at 485/530 nm (ex/em) at time zero and every 15 min for 75 min then every 30 min for 2 h. Data are expressed as fold change of production compared to the negative control.

2.4. Evaluation of intracellular ROS production

Intracellular ROS levels were evaluated using the non-florescent probe DCFH-DA as described previously (Ude et al., 2019b). The diacetate allows for the penetration of DCFH-DA into the cell, which is then cleaved by the cell esterase and oxidized by ROS. Existing studies have varied with respect to the protocol used to assess ROS production using the DCFH-DA assay (*e.g.* DCFH-DA probe concentration, the time point at which ROS production is quantified, and whether cells are preloaded with dye then exposed to NMs or exposed to NMs then the DCFH-DA probe) (Karlsson et al., 2008; Lipovsky et al., 2009; Chairuangkitti et al., 2013; Boyles et al., 2016). The DCFH-DA concentration and time point were optimized for the Caco-2 cells and CuO NMs and identified to be 150 μM and 2 h respectively. For cellular ROS production, undifferentiated Caco-2 cells were cultured for 24 h in 96 well plates and, differentiated Caco-2 cells, Caco-2/HT29-MTX and Caco-2 Raji B co-cultures were cultured in transwell plates as described above. Cell

were washed twice and 150 μM DCFH-DA (in HBSS) was added into each of the wells. The cells were incubated for 1 h in the dark at 37 °C, 5% CO_2 and 95% humidity. Cells were then washed twice with PBS and exposed to HBSS (control), H_2O_2 (1 mM), CuO NMs or $CuSO_4$ (3.17, 6.34 or 12.68 Cu μg/cm^2) diluted in HBSS in triplicate and incubated at 37 °C, 5% CO_2 and 95% humidity for 2 h. Fluorescence was then measured at time 0 and after 2 h at 485/530 nm (excitation/emission) using a SpectraMax M5 microplate reader (California USA). Data are expressed as mean fold change of the production compared to the negative control.

2.5. Gene expression studies

Undifferentiated Caco-2 cells, differentiated Caco-2 cells, Caco-2/HT29-MTX and Caco-2/Raji B co-cultures were exposed to DMEM complete cell culture medium (control), 3.17, 6.34 and 12.68 Cu μg/cm^2 of CuO NMs or $CuSO_4$ (100 μl for undifferentiated cells and 500 μl for differentiated cells and co-cultures) and incubated for 4, 12 or 24 h at 37 °C. The treatments were removed, and the cells were washed twice with PBS followed by addition of trypsin EDTA into the wells (100 μl) and incubated for 5 min at 37 °C. Trypsinisation was stopped by addition of complete DMEM cell culture medium (500 μl). The cells were transferred to 1.5 ml Eppendorf tubes and centrifuged for 5 min at 375 *g* using an Eppendorf refrigerated microcentrifuge 5424 (Cole- Palmer UK). The cell pellets were washed in PBS and re-suspended in PBS (30 μl) and ribonucleic acid (RNA) isolated using a MagMAX™ 96 Total RNA Isolation Kit (Ambion, USA) following the manufacturer's protocol. The RNA concentration and purity were measured with a Nanodrop 2000c system (Thermo Scientific, UK) and only isolated RNA samples with a A260/A280 ratio of 2 to 2.1 were used for (complementary deoxyribonucleic acid (cDNA) synthesis. The RNA (900 ng) was transcribed to cDNA using a Precision nanoScript™2 Reverse Transcription kit (Primerdesign, UK) following the manufacturer's protocol.

Real time quantitative polymerase chain reaction (RT qPCR) analysis was performed with a 7900 RT fast PCR system and SDS 2.3 software with 384 well plates (Applied Biosystems, USA), using a custom designed real-time PCR assay with Double-Dye probe and Precision PLUS qPCR Master Mix (Primerdesign, UK) following the manufacturer's instructions. cDNA (25 ng) was used for RT qPCR. Activation, denaturation and data collection were carried out at 95 °C for 2 min, 95 °C for 10s and 60 °C for 1 min respectively for 40 cycles. Glyceraldehyde 3- phosphate dehydrogenase (GAPDH) was used as an internal control/housekeeping gene as GAPDH has been identified previously as being the best housekeeping gene for the Caco-2 cell (*e.g.* Piana et al., 2008; Vreeburg et al., 2011). Non-reverse transcribed RNA control was also included and processed the way the test samples were prepared. The fluorogenic data was collected and analysed using SDS v2.4.1 software (Applied Biosystems, USA). Sequences of primers supplied by primer design (Primerdesign, UK) are as follows: *IL8*: sense, 5′-CAGAGACAGCAGAGCACAC-3′, anti-sense, 5′-AGCTTGGAAGTCATGTTTACAC-3′ *HMOX1*; sense, 5′-GGAAGCCCCCACTCAACA-3′ Anti-sense, 5′-GCATAAAGCCCTACAGCAACT-3′; *MUC2*: sense, 5′-ACCTCCATCAATAACTCCTCCTA-3′, antisense, 5′-CTCCACCTGGTTTGTGAAAGT-3′; *MT1A*: sense, 5′-GCCCTGCTCGAAGATATAGAAAG-3′, anti-sense, 5′-AATACAGTAAATGGGTCAGGGTT-3′ and *MT2A*: sense, 5′-GACTCTAGCCGCCTCTTCAG-3′ anti-sense 5′-GGCAGCAGGAGCAGCAG-3′. Data are expressed as mean fold change in gene expression (compared to the control).

2.6. Intracellular HMOX-1 protein level

Undifferentiated Caco-2 cells were cultured for 24 h in 24 well plates (Costar Corning, Flintshire, UK) and differentiated Caco-2 cells, Caco-2/HT29-MTX and Caco-2 Raji B co-cultures were cultured in transwell plates as described above. Cells were washed twice with PBS and exposed to DMEM complete cell culture medium (control), H_2O_2 (1 mM), CuO NMs or $CuSO_4$ (6.34 or 12.68 Cu μg/cm^2) diluted in DMEM complete cell culture medium and incubated at 37 °C, 5% CO_2 and 95% humidity for 24 h. The cell culture medium was removed, and cells lysed following the protocol described in R&D systems DuoSet IC ELISA kit. The cell lysates were then assessed for HMOX-1 production using the Enzyme-linked Immunosorbent Assay (DuoSet IC ELISA kit), (R&D Systems, Abingdon, UK) following the manufacturer's protocol. The absorbance was measured using a SpectraMax M5 microplate reader (California USA) at wavelength 450 nm and the HMOX-1 production calculated from the standard curve and expressed in pg/ml.

2.7. Data analysis

Each experiment was repeated at least three times (on different days) and all data generated from these experiments are expressed as the mean ± standard error of the mean (SEM). The figures were generated using Graph Pad Prism. After checking normality of the data, a one-way analysis of variance (ANOVA) and the Tukeys multiple comparison *post hoc* test was employed to investigate statistical significance using Minitab 17 software.

3. Results

3.1. Impact of CuO NMs and $CuSO_4$ on ROS production

In acellular conditions, both CuO NMs and $CuSO_4$ increased ROS production at all concentrations tested and in a concentration dependent manner (Fig. 1A). The greatest increase in ROS production was observed at the highest concentration of 12.68 Cu μg/cm^2 for both CuO NMs and $CuSO_4$. However, the level of ROS production stimulated by $CuSO_4$ was double that observed for CuO NMs at concentrations of 3.17 and 6.34 Cu μg/cm^2 and more than three-fold higher at the highest concentration of 12.68 Cu μg/cm^2 (Fig. 1A).

Following exposure of undifferentiated Caco-2 cells, differentiated Caco-2 cells, and Caco2/HT29-MTX and Caco-2/Raji B co-cultures to CuO NMs for 2 h, no significant increase in ROS formation was observed, compared to control (Fig. 1B–E). However, $CuSO_4$ demonstrated a significant concentration dependent increase (7 to 8-fold increase) in ROS production in undifferentiated Caco-2 cells (Fig. 1B). In differentiated Caco-2 cells and the Caco-2/HT29-MTX co-culture exposed to $CuSO_4$, a 3- and 4-fold increase in ROS production was also observed and a 5 to 7-fold increase was observed in the Caco-2/Raji B co-cultures (Fig. 1).

3.2. Impact of CuO NMs and $CuSO_4$ on HMOX1 gene expression

The influence of CuO NM and $CuSO_4$ concentration on *HMOX1* gene expression was assessed at 4, 12 and 24 h post exposure (Fig. 2). No significant ($P < 0.05$) change was observed in the level of *HMOX1* expressed by CuO NMs and $CuSO_4$. A concentration dependent increase in *HMOX1* expression was observed in all cell models, at all-time points with increasing gene expression observed with increasing concentration. The greatest change in expression was observed at 12 h post exposure in all cell models. The response of undifferentiated Caco-2 cells was the greatest, with up to 78-fold increases in gene expression observed, for the other models about 6 to 9-fold increase was observed. At 12 h the ranking of *HMOX1* expression in each cell model from highest to lowest are as follows: undifferentiated Caco-2 cells > Caco-2/HT29-MTX co-culture > Caco-2/Raji B co-culture > differentiated Caco-2 cell (Fig. 2).

3.3. Impact of CuO NMs and $CuSO_4$ on IL8 gene expression

The impact of CuO NM and $CuSO_4$ concentration on *IL8* gene expression was investigated at 4, 12 and 24 h (Fig. 3A–D). CuO NMs and $CuSO_4$ stimulated the greatest level of IL8 expression in undifferentiated Caco-2 cells, with a 247-fold increase at the highest concentration of 12.68 Cu μg/cm^2 after 12 h post exposure and differentiated Caco-2 cells had the lowest expression (6-fold increase) (Fig. 3A–D). At 24 h post

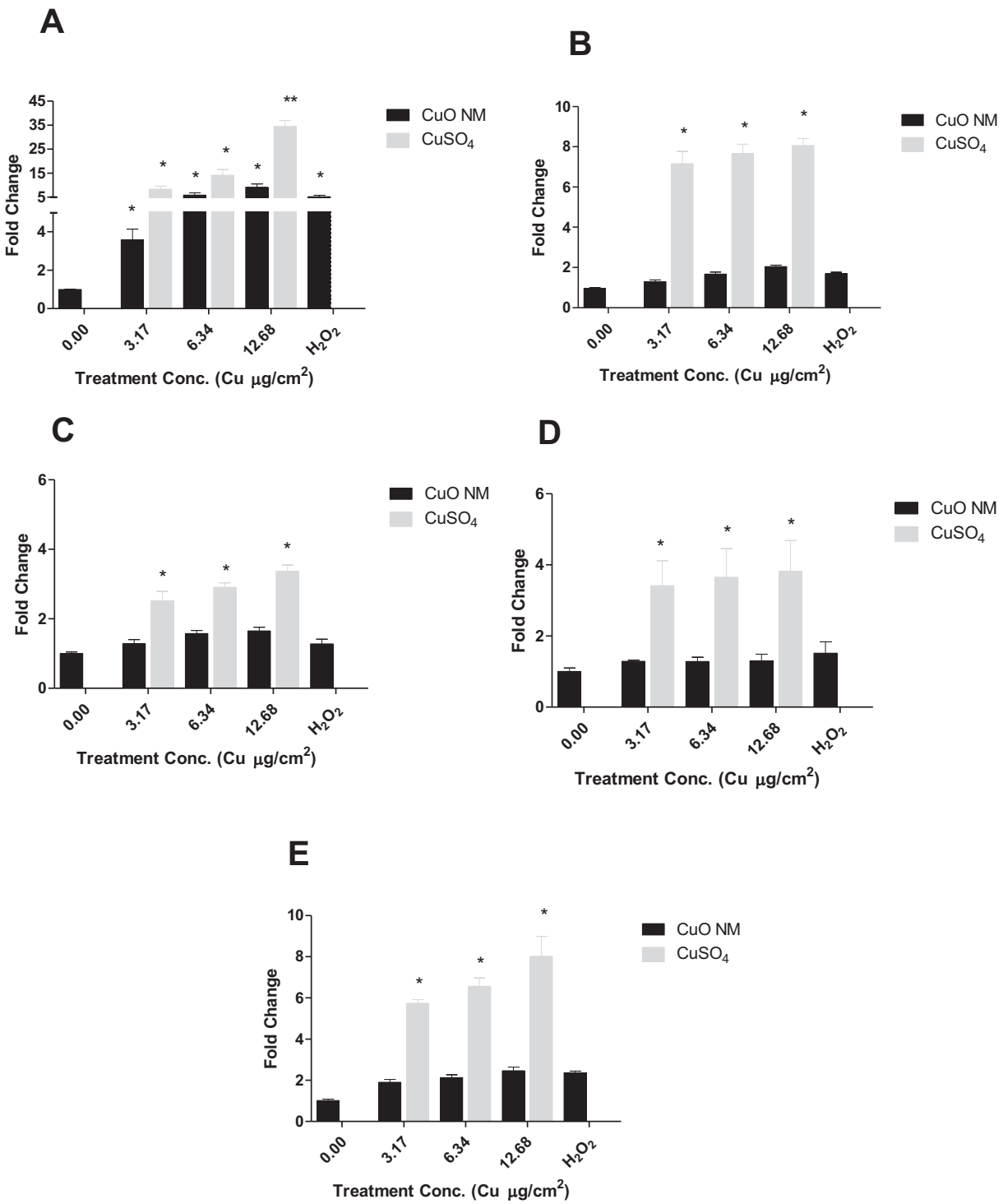

Fig. 1. Acellular and cellular ROS formation at 2 h post exposure to CuO NMs and $CuSO_4$. Acellular ROS production determined using the DCFH-DA assay exposed for 2 h to CuO NMs and $CuSO_4$(A). Phenol red free MEM complete cell culture medium was included as a negative control and H_2O_2 (1 mM) as a positive control. Intracellular ROS production by undifferentiated Caco-2 cells (B), differentiated Caco-2 cells (C), the Caco-2/HT29-MTX co-culture (D) and the Caco-2/Raji B co-culture (E) following exposure to HBSS (0), 1 mM H_2O_2, CuO NMs and $CuSO_4$ using the DCFH-DA assay at 2 h are also presented. Data are expressed as mean fold change of fluorescent intensity (compared to the negative control) ± SEM ($n = 3$). Significance are indicated by * $P < 0.05$ and ** $= P < 0.01$ compared to control. (For interpretation of the references to colour in this figure legend, the reader is referred to the web version of this article.)

exposure, the greatest increase in *IL8* expression was observed in undifferentiated Caco-2 cells, with a fold change of 115 and the lowest in Caco-2/Raji B co-culture (4-fold) (Fig. 3A–D). At 12 h post exposure the ranking of *IL8* expression in the models from highest to lowest are follows: undifferentiated Caco-2 cells>Caco-2/Raji B co-culture>Caco-2/HT29-MTX co-culture>differentiated Caco-2 cells (Fig. 3).

3.4. Impact of CuO NMs and $CuSO_4$ on metallothionein gene expression

Exposure of undifferentiated Caco-2 cells to CuO NMs and $CuSO_4$ at concentrations of 3.17, 6.34 and 12.68 Cu µg/cm^2 for 4, 12 and 24 h did not show a significant increase in *MT1A* gene expression (Fig. 4A). However, a significant time and concentration dependent increase in

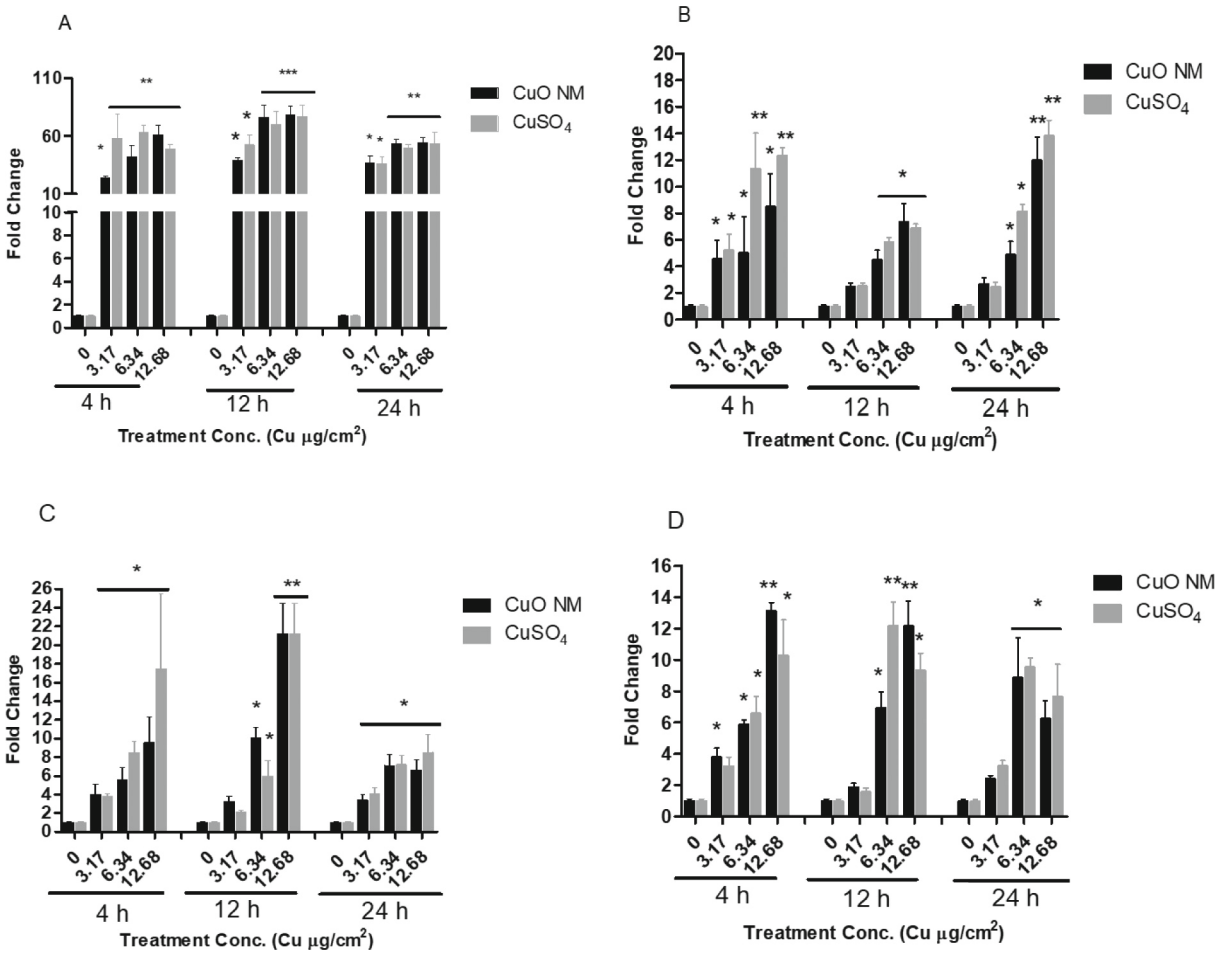

Fig. 2. *HMOX1* expression stimulated by CuO NMs and $CuSO_4$ in *in vitro* intestinal models of varied complexity. Cells were exposed to cell culture medium (control, 0), CuO NMs or $CuSO_4$ at concentrations of 3.17, 6.34 or 12.68 Cu µg/cm^2 for 4, 12 or 24 h and *HMOX1* expression was assessed in undifferentiated Caco-2 cells (A), differentiated Caco-2 cells (B), Caco-2/HT29-MTX (C) and Caco-2/Raji B (D) co-cultures. Data are expressed as mean fold-change in gene expression (compared to control) ± SEM ($n = 3$). Significance is indicated by * $P < 0.05$, ** $P < 0.01$, ***$P < 0.001$, compared to the negative control (0).

MT1A expression was observed in differentiated Caco-2 cells, Caco-2/HT29-MTX and Caco-2/Raji B co-cultures (Fig. 4A–D). At 12 h post exposure to CuO NMs and $CuSO_4$, the Caco-2/HT29-MTX co-culture demonstrated the highest expression of *MT1A* (13-fold) and undifferentiated Caco-2 cells showed the lowest expression (3-fold) (Fig. 4A–D). At 24 h post exposure of CuO NMs and $CuSO_4$, the greatest MT1A expression was observed in differentiated Caco-2 cells (23-fold), and the lowest expression was observed in undifferentiated Caco-2 cells (2.5-fold) (Fig. 4A–D). At 12 h post exposure the ranking of *MT1A* expression in the models from highest to lowest are follows: Caco-2/HT29-MTX co-culture>differentiated Caco-2 cells>Caco-2/Raji B co-culture> undifferentiated Caco-2 cells (Fig. 4).

On exposure of differentiated Caco-2 cells, Caco-2/HT29-MTX and Caco-2/Raji B co-cultures to CuO NMs and $CuSO_4$ at concentration of 3.17, 6.34 and 12.68 Cu µg/cm^2 for 4, 12 and 24 h, a concentration and time dependent increase in *MT2A* expression was observed. The highest level of *MT2A* expression was observed in the Caco-2/HT29-MTX co-culture with fold change of 14, followed by differentiated Caco-2 cells (4-fold) and then Caco-2/Raji B co-culture (4-fold) at 12 h post exposure (Fig. 5A–C). However, at 24 h differentiated Caco-2 cells demonstrated the highest expression of *MT2A* with a fold change of 23, followed by Caco-2/HT29-MTX co-culture (14-fold) and Caco-2/Raji B co-culture (3-fold) (Fig. 5A–C). The fold change was not calculated for *MT2A* expression by undifferentiated Caco-2 cells because the untreated control did not express *MT2A* at a detectable level. Therefore, the results are presented as threshold cycle (Ct) values in Table 1. Since the untreated control did not express *MT2A* at a detectable level (Ct value >40), it can be deduced that CuO NMs and $CuSO_4$ increased *MT2A* expression at all concentrations and time points tested. However, there was no significant change in Ct values across the concentrations at all time points (Table 1).

3.5. Impact of CuO NMs and $CuSO_4$ on MUC2 expression

A concentration dependent increase in *MUC2* expression was observed at 4, 12 and 24 h post exposure of CuO NMs and $CuSO_4$ at highest concentration tested (Fig. 6A–D). The greatest expression was observed in undifferentiated Caco-2 cells with a fold increase of 26 at concentration of 12.68 Cu µg/cm^2, followed by Caco-2/Raji B co-culture (4.5 fold), then differentiated Caco-2 cells (4.2 fold) and Caco-2/HT29-MTX co-culture (3.5 fold) at 12 h (Fig. 6A–D). Whilst at 24 h post exposure, the greatest expression was observed in differentiated Caco-2 cells (28-fold) followed by Caco-2/HT29-MTX co-culture (16-fold), undifferentiated Caco-2 cells (4.5-fold) and Caco-2/Raji B co-culture (3.7 fold) (Fig. 6A–D). Caco-2/HT29-MTX co-culture control had the lowest *MUC2* Ct value compared to other cell models at all time points (result not shown) which is an indication that Caco-2/HT29-MTX co-culture induced greater expression of *MUC2* compared to other *in vitro* cell models used in this study. At 12 h post exposure the ranking of *MUC2* expression in the models from highest to lowest are as follows: undifferentiated Caco-2 cells>differentiated Caco-2 cells> Caco-2/HT29-MTX co-culture>Caco-2/Raji B co-culture (Fig. 6).

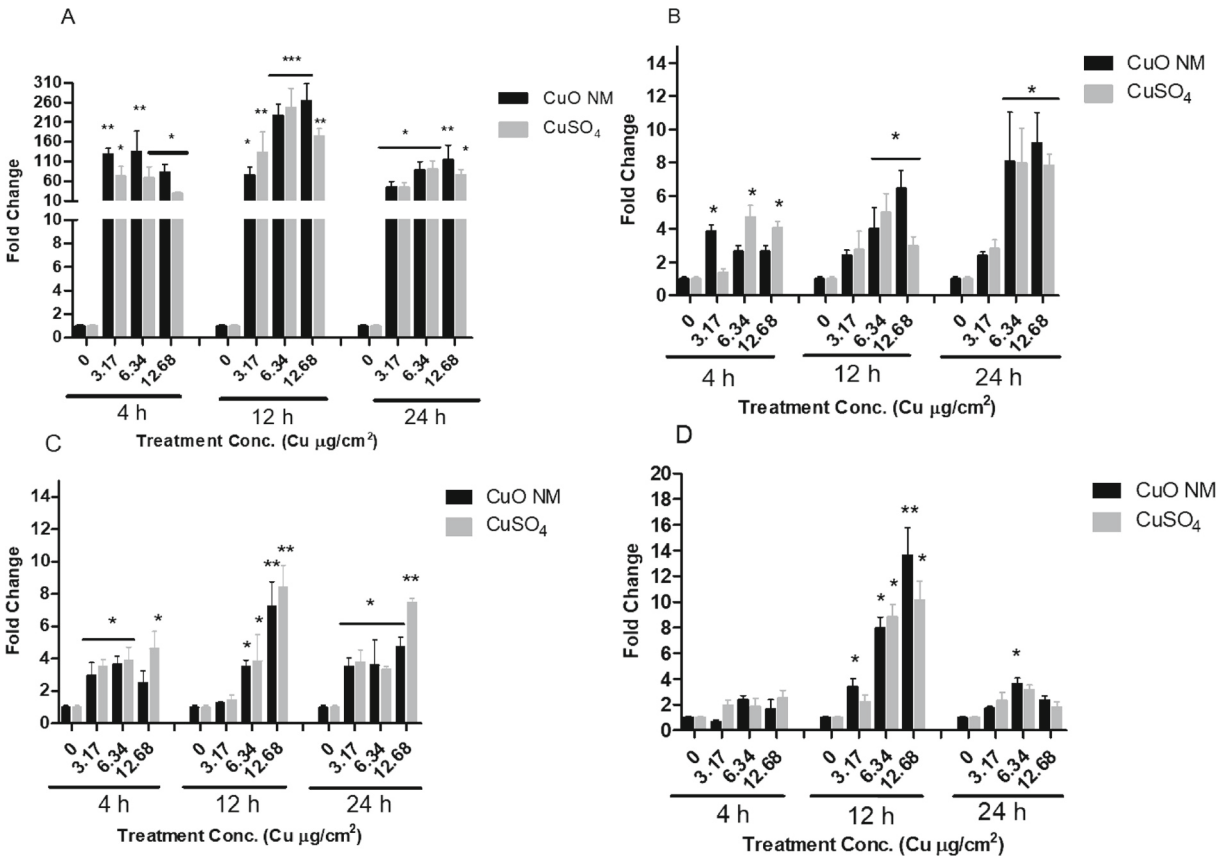

Fig. 3. *IL-8* expression stimulated by CuO NMs and $CuSO_4$ in *in vitro* intestinal models of varied complexity. Cells were exposed to cell culture medium (control, 0), CuO NMs or $CuSO_4$ at concentrations of 3.17, 6.34 or 12.68 Cu μg/cm^2 for 4, 12 or 24 h and *IL-8* expression was assessed in undifferentiated Caco-2 cells (A), differentiated Caco-2 cells (B), Caco-2/HT29-MTX (C) and Caco-2/Raji B (D) co-cultures. Data are expressed as mean fold-change in *IL8* expression (compared to control) ± SEM ($n = 3$). Significance are indicated by * $P < 0.05$, ** $P < 0.01$, *** $P < 0.001$ compared to control.

3.6. Intracellular HMOX-1 protein level

A significant ($P < 0.05$) increase in HMOX-1 levels were observed in the cell lysates following exposure of the undifferentiated Caco-2 cells, differentiated Caco-2 cells, Caco-2/Raji B and Caco-2/HT29-MTX co-cultures to CuO NMs and $CuSO_4$ for 24 h, when compared to the control (Fig. 7). Undifferentiated Caco-2 cells demonstrated the highest level of HMOX-1 followed by differentiated, Caco-2/HT29-MTX and Caco-2/Raji B co-cultures. The level of HMOX-1 in cells after exposure to positive control (H_2O_2) was lower than CuO NMs and $CuSO_4$ but was significantly ($P < 0.05$) higher than the negative control (0).

4. Discussion

To investigate the toxicity of sub-lethal exposure of intestinal *in vitro* models to CuO NMs and $CuSO_4$, the expression of 5 genes associated with oxidative stress (*HMOX1*), metal binding (*MTIA* and *MT2A*), inflammatory response (*IL8*) and mucus formation (*MUC2*) were investigated. This study compared the expression of these genes using 4 different intestinal *in vitro* models at 3 timepoints in order to determine and compare the responsiveness of the *in vitro* models to CuO NMs and $CuSO_4$, and to inform the experimental design of subsequent studies with respect to which endpoints, timepoints and models should be prioritised when assessing the toxicity of NMs to the intestine *in vitro*. In addition, the level of HMOX-1 protein was assessed, to identify if changes in *HMOX-1* gene expression corresponded to a change in protein levels in the cells. Investigating the same endpoints across intestinal *in vitro* models of varying complexity can be challenging due to differences in the experimental set up used for each model. For example, assessment of the impact of NMs on barrier integrity *via* TEER measurement and tight junction protein staining can only be measured in differentiated cells that are cultured in transwell plates and is not applicable when using undifferentiated cells. Therefore, we investigated changes in gene expression as this methodology is applicable across all the *in vitro* formats. In addition, investigation of the impact of NM on gene expression can provide useful insights into the mechanism of NM toxicity and can allow relatively quick assessments of NM toxicity to be made (as time points < 24 h can be used).

In this study, it was demonstrated that exposure of all four *in vitro* models to CuO NMs and $CuSO_4$ led to an upregulation of genes that control inflammation (*IL8*), oxidative stress (*e.g. HMOX1*), metal binding (*MT1A* and *MT2A*) and mucus production (*MUC2*) and an increase in the level of the HMOX-1 protein. However, although the pattern of response was similar across all models, the upregulation of some of the genes (*HMOX1* and *IL8*) was much higher in the undifferentiated cells than the differentiated cell models and some of the genes (*HMOX1* and *IL8*) can be detected at earlier timepoint (4 h) in undifferentiated Caco-2 cell Although both CuO NMs and $CuSO_4$ generated ROS in a cell free environment, only $CuSO_4$ mediated ROS production in the cell models. The response to $CuSO_4$ was significant in all cell models with undifferentiated Caco-2 cell showing greatest ROS production followed by Caco-2/Raji B co-culture, Caco-2/HT29-MTX co-culture and differentiated Caco-2 cells.

4.1. ROS production

NMs can exhibit toxicity *via* stimulation of an oxidant response (Fu et al., 2014; Sabella et al., 2014; Abdal Dayem et al., 2017; Johnston

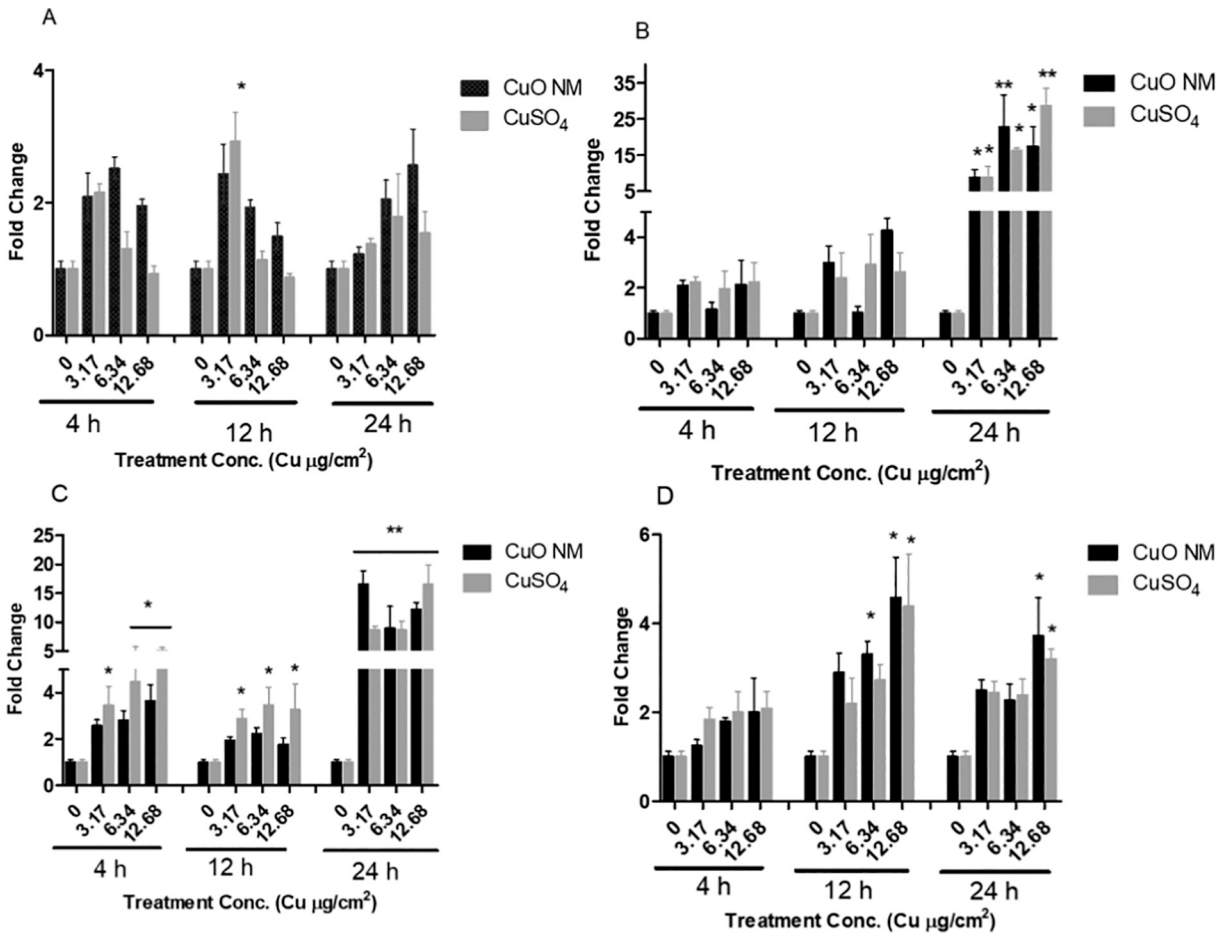

Fig. 4. *MT1A* expression stimulated by CuO NMs and $CuSO_4$ in *in vitro* intestinal models of varied complexity. Cells were exposed to cell culture medium (control, 0), CuO NMs or $CuSO_4$ at concentrations of 3.17, 6.34 or 12.68 Cu μg/cm^2 for 4, 12 or 24 h and *MT1A* expression was assessed in undifferentiated Caco-2 cells (A), differentiated Caco-2 cells (B), Caco-2/HT29-MTX (C) and Caco-2/Raji B (D) co-cultures. Data are expressed as mean fold-change in *MT1A* expression (compared to control) ± SEM ($n = 3$). Significance are indicated by * $P < 0.05$, compared to control.

et al., 2018). For example, there is evidence that ZnO, CNTs, ultrafine carbon black, TiO_2 and Ag NMs can stimulate ROS production in a range of cell types (*e.g.* human keratinocytes, Caco-2 cells, macrophages and immortalized brain microglia) (Stone et al., 2000; Long et al., 2006; Ryu et al., 2014; Chen et al., 2016). As the cellular responses activated by NMs commonly involve the enhanced production of ROS, and ROS production is used as an indicator of NM reactivity (Peijnenburg et al., 2020), acellular and cellular ROS production was also assessed. CuO NMs have previously been shown to stimulate ROS production in alveolar epithelial cells (A549), hepatocellular carcinoma (HCC), hepatocytes (HepG2, (SK-Hep-1) and airway epithelial (HEp-2) cells (Fahmy and Cormier, 2009; Wang et al., 2012; Kung et al., 2015). Previous studies have also demonstrated that in A549 cells CuO NMs stimulated the greatest increase in ROS production compared to NMs of TiO_2, ZnO, $CuZnFe_2O_4$, Fe_3O_4 and Fe_2O_3 (Karlsson et al., 2008; Boyles et al., 2016). Interestingly, in this study, CuO NMs and $CuSO_4$ produced a significant increase in ROS production in acellular conditions. $CuSO_4$ produced more ROS compared to the CuO NMs which is likely to derive from the fact that CuO NMs are not 100% soluble at the time point investigated (Ude et al., 2017).

In this paper, in cellular conditions, only $CuSO_4$ induced a significant increase in ROS production, which is likely to be because CuO NMs are not 100% soluble at the time point and that only ionic form of Cu can induce ROS production. A similar result was reported by Li et al. (2020), when differentiated Caco-2 cells were exposed to CuO NMs (diameter < 50 nm). Longer time points were not used for this study as ROS production was assessed using HBSS which does not support cell growth and ROS production after 2 h. When phenol free medium was used to investigate ROS production in Caco-2 cells after exposure to CuO NMs, no response was observed (data not shown). Undifferentiated Caco-2 cells produced the greatest level of ROS after exposure to $CuSO_4$ followed by Caco-2/Raji B co-culture, Caco-2/HT29-MTX co-culture then, differentiated Caco-2 cells. The greatest response observed in undifferentiated cells aligns with our previous studies, and those of the wider scientific community (Gerloff et al., 2013; Ude et al., 2017). $CuSO_4$ demonstrated greater ROS production in all the intestinal cell models than the positive control (H_2O_2), suggesting that $CuSO_4$ may be a better ROS chemical (positive) control in intestinal cell culture models than H_2O_2.

4.2. Gene expression

An upregulation of *HMOX1* expression in cells suggest that there has been an increase in ROS production. Various reports have demonstrated an upregulation of *HMOX1* expression in a variety of cell types to NM exposure. For example, Ag NMs (5–37 nm) upregulated *HMOX1* expression after exposure of HeLa and A549 cells (Miura and Shinohara, 2009; Sthijns et al., 2017), while ZnO NMs upregulated *HMOX1* expression in a monoculture of A549 cells and a co-culture of A549 and human coronary artery endothelial cells (HCAECs) (Yan et al., 2017). An increase in *HMOX1* expression was shown in Caco-2 cells after exposure to Au NMs (Bajak et al., 2015) and CuO NMs upregulated *HMOX1* expression in the A549 and HepG2 cell line (Cuillel et al., 2014; Strauch et al., 2017). SiO_2 NMs were also shown to upregulate *HMOX1*

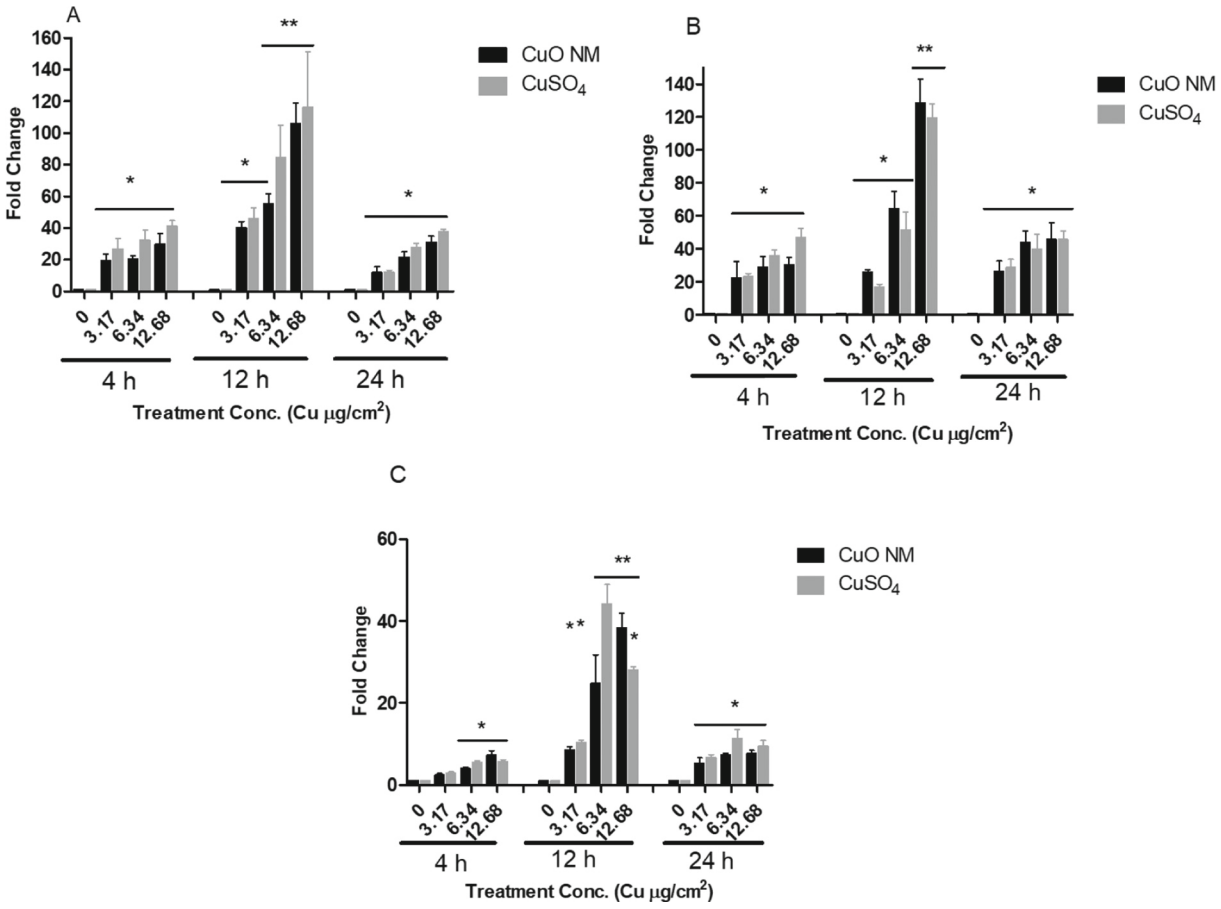

Fig. 5. *MT2A* expression stimulated by CuO NMs and $CuSO_4$ in *in vitro* intestinal models of varied complexity. Cells were exposed to cell culture medium (control, 0), CuO NMs or $CuSO_4$ at concentrations of 3.17, 6.34 or 12.68 Cu μg/cm^2 for 4, 12 or 24 h and *MT2A* expression was assessed in differentiated Caco-2 cells (A), Caco-2/HT29-MTX (B) and Caco-2/Raji B (C) co-cultures. Data are expressed as mean fold-change in *MT2A* expression (compared to control) ± SEM (n = 3). Significance are indicated by * $P < 0.05$, ** $P < 0.01$, compared to control.

Table 1
Effect of CuO NMs and $CuSO_4$ on *MT2A* expression in undifferentiated Caco-2 cells *MT2A* expression. Undifferentiated Caco-2 cells were exposed to cell culture medium (control, 0), CuO NMs or $CuSO_4$ at concentrations of 3.17, 6.34 or 12.68 Cu μg/cm^2 for 4, 12 and 24 h.

Time (h)	CuO NMs (Cu μg/cm^2)			$CuSO_4$ (Cu μg/cm^2)		
	3.17	6.34	12.68	3.17	6.34	12.68
4	18.84 ± 0.69	17.37 ± 0.31	17.19 ± 0.47	17.49 ± 0.36	18.26 ± 0.74	18.89 ± 0.50
12	18.23 ± 0.22	17.30 ± 0.27	17.96 ± 0.38	18.14 ± 0.25	18.34 ± 0.21	19.67 ± 0.37
24	17.88 ± 0.55	18.05 ± 0.66	17.96 ± 0.38	17.78 ± 0.55	18.74 ± 0.58	19.47 ± 0.41

Data are expressed as mean Ct value ± SEM ($n = 3$). Gene expression was not detected for the control (Ct value > 40), and none of the values measured at different treatment concentrations or time were statistically significant compared to the control.

expression in HaCat cell line but not in Caco-2 cells (Ebabe Elle et al., 2016). Exposure of graphene oxide and graphene nanoplatelets to differentiated Caco-2 cells, and a Caco-2/HT29 co-culture have also shown low inflammatory response and lack of ROS production and *HMOX1* gene expression suggesting that the nanoplatelets were not toxic to both cell models (Domenech et al., 2020a; Domenech et al., 2020b). There is therefore evidence from multiple studies that upregulation of *HMOX1* gene expression is associated with exposure of various cell types to NMs of varied physico-chemical properties.

In this study, CuO NMs and $CuSO_4$ caused a concentration and time dependent increase in *HMOX1* gene expression in all cell models, with undifferentiated Caco-2 cells showing the greatest response which is similar to the intracellular HMOX-1 protein assay assessed using ELISA after 24 h. Therefore, investigation of *HMOX1* expression at 4 h post exposure may be suggested in future studies. The greatest upregulation in *HMOX1* by undifferentiated Caco-2 cells suggests their greater susceptibility to toxicity compared to the differentiated Caco-2 cells and the co-cultures. It was unexpected that the increase in *HMOX1* expression was not associated with an increase in ROS production in cells but increase in gene expression corresponded to HMOX-1 protein level.

MT proteins are known to possess metal detoxifying properties and have the ability to scavenge excess metals (Sahu et al., 2013). CuO NMs have been shown to upregulate *MT2A* expression in human bronchial epithelial (BEAS-2B) cells (Strauch et al., 2017) and a marked upregulation in *MT2A* expression has been reported after exposure of the HeLa cell line to Ag NMs, which was attributed to oxidative stress (Miura and Shinohara, 2009). ZnO and Ag NMs have also been shown to upregulate *MT1A* and *MT2A* in A549 alveolar epithelial cells (Dekkers et al., 2018).

Our data indicates that *MT2A* was significantly upregulated following exposure to CuO NMs and $CuSO_4$ at all concentrations and time points in all intestinal *in vitro* models, hence *MT2A* expression may be investigated at 4 h post exposure of NMs in future. Although *MT1A* expression was high compared to *MT2A* before CuO NMs and $CuSO_4$ exposure, after treatment the level of *MT1A* expression did not increase to the same extent as *MT2A*, suggesting that *MT2A* is more sensitive to CuO NMs and $CuSO_4$ than *MT1A* in all cell models used. The level of *MT2A* expression induced by CuO NMs and $CuSO_4$ was similar in all

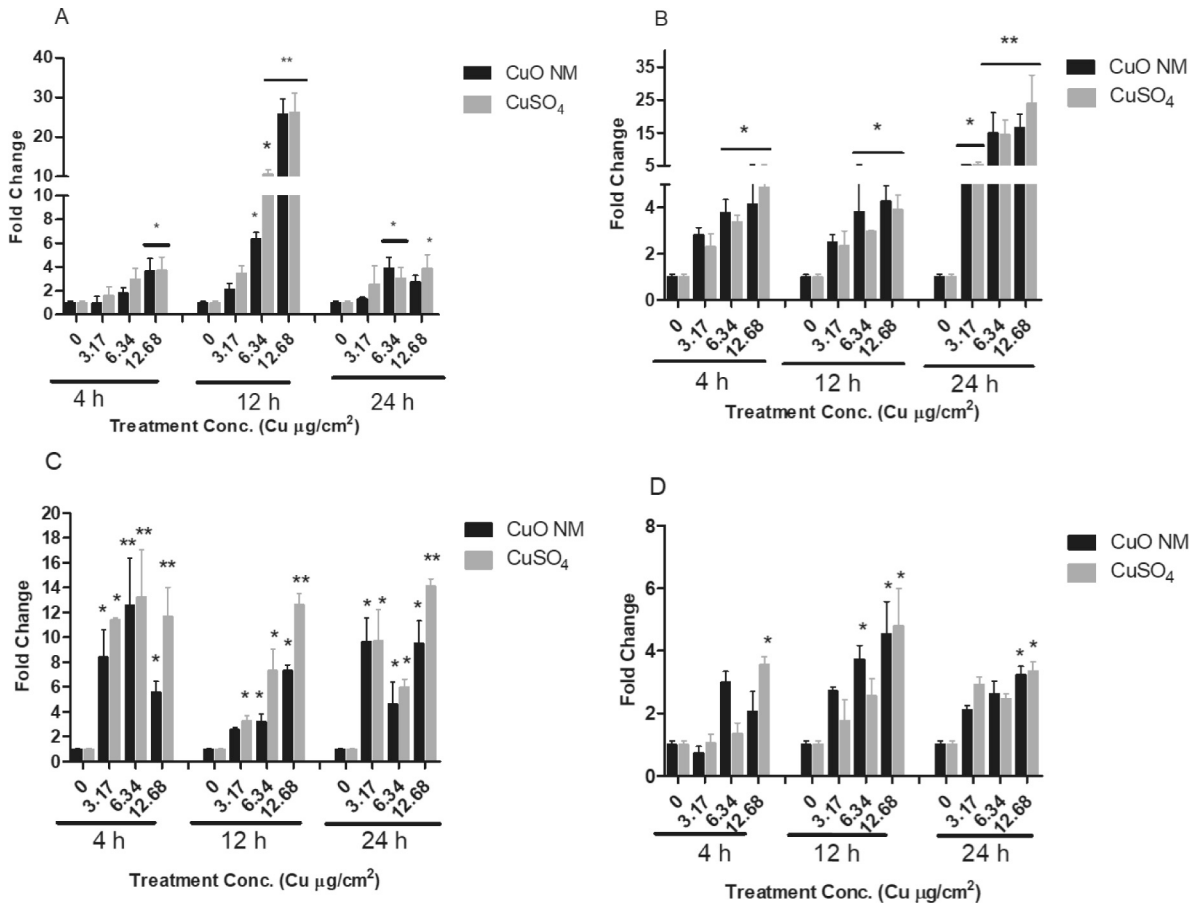

Fig. 6. *MUC2* expression stimulated by CuO NMs and $CuSO_4$ in *in vitro* intestinal models of varied complexity. Cells were exposed to cell culture medium (control, 0), CuO NMs or $CuSO_4$ at concentrations of 3.17, 6.34 or 12.68 Cu μg/cm^2 for 4, 12 or 24 h and *MUC2* expression was assessed in undifferentiated Caco-2 cells (A), differentiated Caco-2 cells (B), Caco-2/HT29-MTX (C) and Caco-2/Raji B (D) co-cultures. Data are expressed as mean fold-change in *MUC2* expression (compared to control) ± SEM ($n = 3$). Significance are indicated by * $P < 0.05$, ** $P < 0.01$, compared to control.

models except undifferentiated Coco-2 cells where the fold change was not calculated due to a lack of *MT2A* expression in the control. Therefore, it may be suggested that undifferentiated Caco-2 cells may not be used when studying *MT2A* expression as it may not allow for calculation of fold change.

Induction of *MT* genes is likely because of the presence of copper ions in the cells. These ions may have been generated either from dissociated CuO NMs prior to uptake or after internalisation by cells. Previous studies have shown that when soluble NMs are internalised by cells in a particle form, they tend to dissociate intracellularly (in acidic lysosomes), thereby exhibiting a Trojan horse-type mechanism of toxicity (Cho et al., 2011; Shinohara et al., 2017). Internalised Ag NMs dissociated intracellularly in an immortalized murine microglial cell line (BV-2) inducing toxicity *via* a Trojan horse mechanism in a previous research (Hsiao et al., 2015). Therefore, it is hypothesized that CuO NMs release Cu ions inside cells which binds to MTs and promotes MT gene expression. Our previous studies quantified Cu uptake by cells (using ICP-OES) (Ude et al., 2017, 2019a), but further studies would be required to investigate their intracellular fate to help confirm this hypothesis.

IL-8 protein is secreted at sites of inflammation and has been shown to be responsible for stimulating increased recruitment and migration of neutrophils (Struyf et al., 2005). Expression of *IL8* at 4 h has been reported after exposure of undifferentiated Caco-2 cells to ZnO and SiO_2 NMs (Gerloff et al., 2013). TiO_2 has also been reported to induce transient *IL8* gene expression in Caco-2 cells (Krüger et al., 2014). This study demonstrated a significant upregulation of *IL8* expression by CuO NMs and $CuSO_4$ at all concentrations and time points tested. Therefore, *IL8* expression may be investigated at 4 h post exposure to NMs in all cell models. Previously, the CuO NMs and $CuSO_4$ used for this study have been shown to stimulate a significant increase in IL-8 protein production at 24 h post exposure to undifferentiated Caco-2 cells, differentiated Caco-2 cell, Caco-2/Raji B and Caco-2/HT29-MTX co-cultures (Ude et al., 2017; Ude et al., 2019a). Since the expression of *IL8* directly corroborates the previously published IL-8 protein data (Ude et al., 2017; Ude et al., 2019a), this suggests that gene expression could be a way to reduce the time needed to study the toxic effect of NM to the intestine using *in vitro* models. In addition, undifferentiated Caco-2 cells demonstrated a greater level of *IL8* expression compared to the differentiated Caco-2 cells and co-cultures which also corroborates with our previous study which demonstrated a greater secretion of IL-8 protein by undifferentiated Caco-2 cells compared to differentiated Caco-2 cells and co-cultures (Ude et al., 2017; Ude et al., 2019a). The elevated level of *IL8* expression by undifferentiated Caco-2 cells indicates the responsiveness of undifferentiated Caco-2 cells compared to other *in vitro* models used in this study.

Mucin (MUC) is secreted in the goblet cells and acts as a first line of defence in the intestine (Tailford et al., 2015; Tadesse et al., 2017). *MUC2* is the most abundant mucin protein in the intestine and their abnormal expression may lead to deleterious effects (Lee et al., 2015; Tadesse et al., 2017). For example, toxic substances (bisphenol A) which can cause oxidative stress and apoptosis have been reported to reduce *MUC2* expression and eventually lead to intestinal barrier dysfunction (Lee et al., 2015; Zhao et al., 2019). It has also been reported that inflammation may induce increased mucus secretion with dysfunctional viscoelastic properties (Elamin et al., 2014; Cornick et al., 2015). The Caco-2/HT29-MTX co-culture had the greatest *MUC2* expression in the

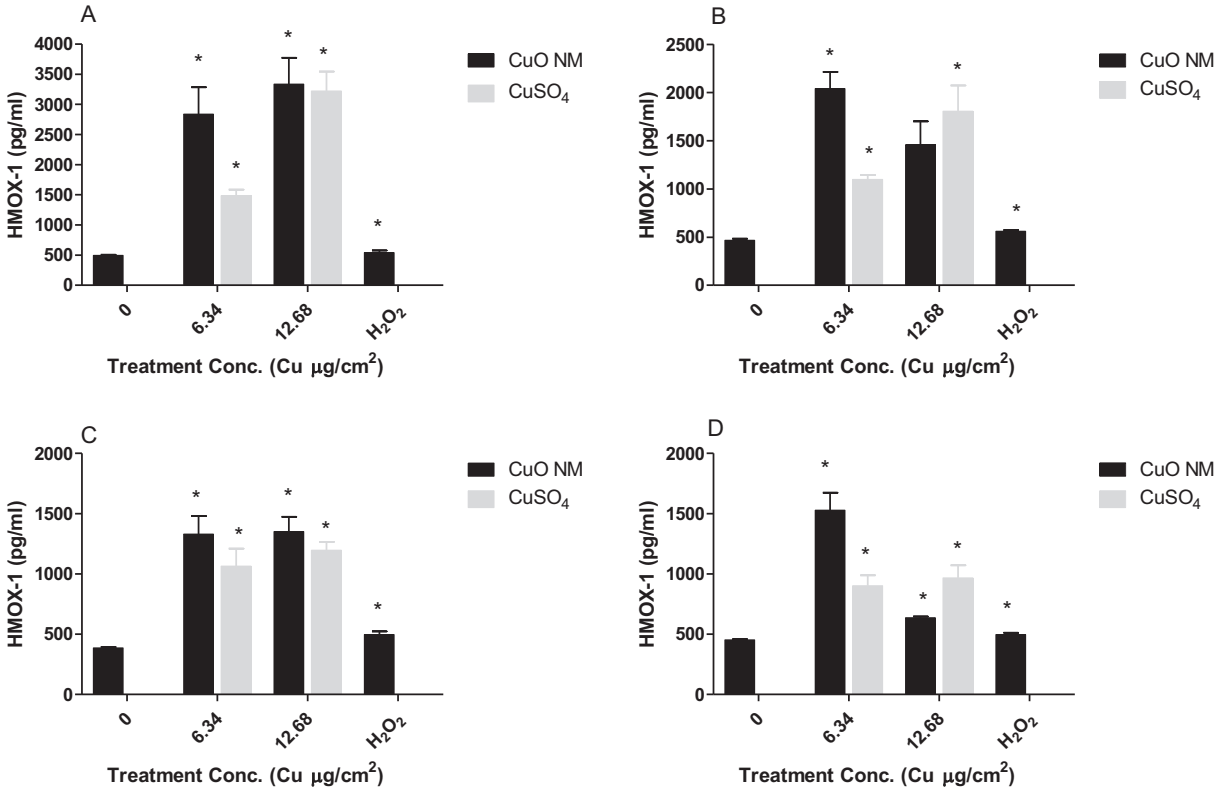

Fig. 7. HMOX-1 protein production induced by CuO NMs and $CuSO_4$ in *in vitro* intestinal models of varied complexity. Cells were exposed to cell culture medium (control, 0), 1 mM H_2O_2, CuO NMs or $CuSO_4$ at concentrations of 6.34 or 12.68 Cu µg/cm^2 for 24 h. HMOX-1 production was assessed in cell lysate of undifferentiated Caco-2 cells (A), differentiated Caco-2 cells (B), Caco-2/HT29-MTX (C) and Caco-2/Raji B (D) co-cultures. Data are expressed as mean HMOX-1 concentration in pg/ml ± SEM. Significance is indicated by * $P < 0.05$ compared to the negative control (0). ($n = 3$).

control group reflecting the presence of the mucus secreting cell line. This suggests that Caco-2/HT29-MTX co-culture may be preferred when impact of mucus on NMs uptake and translocation is being investigated. *MUC2* was also upregulated in a concentration and time dependent manner from 4 to 12 h and decreased at 24 h post exposure to CuO NMs and $CuSO_4$ in undifferentiated Caco-2 cells. However, undifferentiated Caco-2 cells had the greatest expression at 12 h which decreased at 24 h after exposure to CuO NMs and $CuSO_4$. The increased expression of *MUC2* following exposure to CuO NMs and $CuSO_4$ suggests that the cells could have upregulated mechanisms to protect themselves against toxic substances *via* the production of mucus. When the cells ability to protect themselves are supressed by the toxicants, apoptosis will set in followed by reduction in *MUC2* expression, as was observed in undifferentiated Caco-2 cells (the most sensitive model). *MUC2* expression has not been previously investigated for Caco-2 cell responses to NMs, although it has been investigated for other chemicals/pathogens (Azzam et al., 2011; Elamin et al., 2014; Cobo et al., 2015; Zhao et al., 2019). Dorier et al. (2019) reported that exposure of various TiO_2 (E171 (119 nm) A12 (12 nm) and P25 (21 nm)) to Caco-2/HT29-MTX co-culture did not upregulate *MUC2* gene expression. This could be attributed to the relatively low toxicity of TiO_2 NMs compared to CuO NMs, which was supported by the inability of TiO_2 NMs to affect intestinal barrier integrity (Dorier et al., 2019) and cell viability (Dorier et al., 2017). The results from this study suggest that *MUC2* expression could be assessed more routinely when investigating NM toxicity to Caco-2 cells.

4.3. Intracellular HMOX-1 protein level

HMOX-1 is an antioxidant enzyme known to play an important role in protection and preservation of GI tract mucosa from acute and chronic inflammation (Zhu et al., 2011). HMOX-1 has the capability of regulating stress caused by hypoxia, ROS and heat shock (Cooper et al., 2009; Tsuji et al., 2009; Chang et al., 2009). Although, CuO NMs did not cause an increase in ROS production in all the cell models, HMOX-1 increased significantly compared to the control in all the *in vitro* intestinal cell models following exposure to CuO NMs and $CuSO_4$. An increase in the level of *HMOX1* gene expression was also observed in this study in all *in vitro* intestinal models (Section 4.2). Previously, increase in HMOX 1 by CuO NMs but not TiO_2 NMs was observed in a mouse macrophage cell line (Triboulet et al., 2015). Intracellular HMOX-1 has not been studied after exposure of CuO NMs to *in vitro* intestinal models. However, this suggests that intracellular HMOX-1 protein may be a suitable marker for assessment of NM toxicity in the intestine *in vitro*.

5. Conclusion

In this study exposure of all intestinal *in vitro* models tested to CuO NMs and $CuSO_4$ demonstrated a time and concentration dependent upregulation of *HMOX1*, *IL8, MT1A, MT2A* and *MUC2* genes. CuO NMs and $CuSO_4$ also increased HMOX-1 and IL-8 protein in all *in vitro* models, which suggests that assessment of gene expression in these models exposed to NMs are likely useful to predict changes in protein levels. CuO NMs and $CuSO_4$ exhibited ROS production in acellular conditions whereas only $CuSO_4$ mediated ROS production in all four *in vitro* models. In general, the degree of responsiveness, from highest to lowest was ranked: undifferentiated Caco-2 cells > differentiated Caco-2 cells > Caco-2/Raji B co-culture > Caco-2/HT29-MTX co-culture. The only exception was for *MT1A* gene expression, where the undifferentiated model was not responsive. This data therefore supports the use of undifferentiated Caco-2 cells for quick assessment of differential toxicity of panel NMs. However, they may be oversensitive for many NMs and endpoints, and so for a more accurate representation of the intestine *in vivo*, we recommended that co-culture models are prioritised. To select a suitable *in vitro* model for NM studies, considerations of the intended use

and/or application of the study are therefore essential (Kämpfer et al., 2020).

The results of this study also suggest a 4 and 12 h exposure of differentiated Caco-2 cells, Caco-2/Raji B and Caco-2/HT29-MTX co-cultures to NMs is suitable when studying toxicity *via* changes in *HMOXI*, *1 L8* and *MT2A* expression. While for *MT1A* and *MUC2*, 12 h exposure is needed, as this is when a visible increase in response occurred. Although CuO NMs induced *HMOX1* and *MT2A* up regulation, ROS production was not observed in cellular condition at 2 h post exposure in all the *in vitro* models. Therefore, the mechanism of CuO NMs may involve excessive binding of Cu ion to the metallothionein thiol group leading to increased expression of metallothionein gene. Future studies could include antioxidants to assess the role of ROS in this mechanism. In addition, expression of a wider variety of genes such as catalase, glutathione peroxidase, superoxide dismutase, apoptosis genes (caspases 3 and 7) may help to further elucidate the mechanism of CuO NM toxicity. Future studies (*e.g.* https://www.patrols-h2020.eu/) will investigate the toxicity of NMs using triple culture (consisting of epithelial, mucus secreting and immune cells) as well as their applicability for long term studies.

Funding

Tertiary Education Trust Fund (TETFund) Nigeria funded Victor Chibueze Ude's PhD tuition fees and Enugu State University of Science and Technology Enugu, Nigeria granted him study leave. European Union's Horizon 2020 research and innovation programme funded PATROLS project (Grant number 760813) for funding to support the time input of V Stone and H Johnston, and VC Ude when he was writing the paper. All funding bodies had no input in designing the study, collection, analysis, and interpretation of data.

Declaration of Competing Interest

Author declare that they do not have any competing interest.

Acknowledgements

We thank Vice Chancellor of Enugu State University of Science and Technology Enugu Nigeria for granting Victor Chibueze Ude study leave and Tertiary Education Trust Fund Nigeria for funding part of his PhD tuition. We thank the European Union's Horizon 2020 funded project PATROLS (Grant number 760813) for funding to support the time input of V Stone and H Johnston, and VC Ude when his was drafting the manuscript. We thank the SUN EU FP 7 funded project (Grant number 604305) for providing us with CuO NMs.

References

Abbasi-Oshaghi, E., Mirzaei, F., Pourjafar, M., 2019. NLRP3 inflammasome, oxidative stress, and apoptosis induced in the intestine and liver of rats treated with titanium dioxide nanoparticles: *in vivo* and *in vitro* study. Int. J. Nanomedicine 14, 1919–1936.

Abdal Dayem, A., Hossain, M.K., Lee, S.B., Kim, K., Saha, S.K., Yang, G.M., Choi, H.Y., Cho, S.G., 2017. The role of reactive oxygen species (ROS) in the biological activities of metallic nanoparticles. Int. J. Mol. Sci. 18 (1), 120.

Akbari, A., Lavasanifar, A., Wu, J., 2017. Interaction of cruciferin-based nanoparticles with Caco-2 cells and Caco-2/HT29-MTX co-cultures. Acta Biomater. 64, 249–258.

Antunes, F., Andrade, F., Araújo, F., Ferreira, D., Sarmento, B., 2013. Establishment of a triple co-culture *in vitro* cell models to study intestinal absorption of peptide drugs. Eur. J. Pharm. Biopharm. 83 (3), 427–435.

Araújo, F., Shrestha, N., Shahbazi, M.A., Fonte, P., Mäkilä, E.M., Salonen, J.J., Hirvonen, J.T., Granja, P.L., Santos, H.A., Sarmento, B., 2014. The impact of nanoparticles on the mucosal translocation and transport of GLP-1 across the intestinal epithelium. Biomater. 35 (33), 9199–9207.

Azzam, M.M.M., Zou, X.T., Dong, X.Y., Xie, P., 2011. Effect of supplemental l-threonine on mucin 2 gene expression and intestine mucosal immune and digestive enzymes activities of laying hens in environments with high temperature and humidity. Poult. Sci. 90 (10), 2251–2256.

Bajak, E., Fabbri, M., Ponti, J., Gioria, S., Ojea-Jimenez, I., Collotta, A., Mariani, V., Gilliland, D., Rossi, F., Gribaldo, L., 2015. Changes in Caco-2 cells transcriptome profiles upon exposure to gold nanoparticles. Toxicol. Lett. 233 (2), 187–199.

Behrens, I., Stenberg, P., Artursson, P., Kissel, T., 2001. Transport of lipophilic drug molecules in a new mucus-secreting cell culture model based on HT29-MTX cells. Pharm. Res. 18, 1138–1145.

Bhattacharyya, A., Chattopadhyay, R., Mitra, S., Crowe, S.E., 2014. Oxidative stress: an essential factor in the pathogenesis of gastrointestinal mucosal diseases. Physiol. Rev. 94 (2), 329–354.

Boyles, M.S.P., Ranninger, C., Reischl, R., Rurik, M., Tessadri, R., Kohlbacher, O., Duschl, A., Huber, C.G., 2016. Copper oxide nanoparticle toxicity profiling using untargeted metabolomics. Part. Fibre Toxicol. 13 (1), 49.

Bremner, I., 1987. Involvement of metallothionein in the hepatic metabolism of copper. J. Nutr. 117, 19–29.

Bricks, T., Paullier, P., Legendre, A., Fleury, M.J., Zeller, P., Merlier, F., Anton, P.M., Leclerc, E., 2014. Development of a new microfluidic platform integrating co-cultures of intestinal and liver cell lines. Toxicol. in Vitro 28 (5), 885–895.

Brown, D.M., Donaldson, K., Borm, P.J., Schins, R.P., Dehnhardt, M., Gilmour, P., Jimenez, L.A., Stone, V., 2004. Calcium and ROS-mediated activation of transcription factors and TNF-α cytokine gene expression in macrophages exposed to ultrafine particles. Am. J. Phys. 286 (230–2), L344–L353.

Brown, D.M., Dickson, C., Duncan, P., Al-Attili, F., Stone, V., 2010. Interaction between nanoparticles and cytokine proteins: impact on protein and particle functionality. Nanotechnol. 21 (21), 215104.

Brun, E., Barreau, F., Veronesi, G., Fayard, B., Sorieul, S., Chanéac, C., Carapito, C., Rabilloud, T., Mabondzo, A., Herlin-Boime, N., Carrière, M., 2014. Titanium dioxide nanoparticle impact and translocation through *ex vivo*, *in vivo* and *in vitro* gut epithelia. Part. Fibre Toxicol. 11 (1), 13.

Cabellos, J., Delpivo, C., Fernández-Rosas, E., Vázquez-Campos, S., Janer, G., 2017. Contribution of M-cells and other experimental variables in the translocation of TiO_2 nanoparticles across *in vitro* intestinal models. NanoImpact 5, 51–60.

Carpene, E., Andreani, G., Isani, G., 2007. Metallothionein functions and structural characteristics. J. Trace Elem. Med. Biol. 21, 35–39.

Chairuangkitti, P., Lawanprasert, S., Roytrakul, S., Aueviriyavit, S., Phummiratch, D., Kulthong, K., Chanvorachote, P., Maniratanachote, R., 2013. Silver nanoparticles induce toxicity in A549 cells via ROS-dependent and ROS-independent pathways. Toxicol. in Vitro 27 (1), 330–338.

Chang, A.Y., Chan, J.Y., Cheng, H.L., Tsai, C.Y., Chan, S.H., 2009. Hypoxia-inducible factor 1/heme oxygenase 1 cascade as upstream signals in the prolife role of heat shock protein 70 at rostral ventrolateral medulla during experimental brain stem death. Shock 32 (6), 651–658.

Chen, N., Song, Z.M., Tang, H., Xi, W.S., Cao, A., Liu, Y., Wang, H., 2016. Toxicological effects of Caco-2 cells following short-term and long-term exposure to Ag nanoparticles. Int. J. Mol. Sci. 2016 17 (6), 974.

Cho, W.S., Duffin, R., Howie, S.E.M., Scotton, C.J., Wallace, W.A.H., MacNee, W., Bradley, M., Megson, I.L., Donaldson, K., 2011. Progressive severe lung injury by zinc oxide nanoparticles; the role of Zn (2+) dissolution inside lysosomes. Part. Fibre Toxicol. 8, 27.

Civardi, C., Schwarze, F.W., Wick, P., 2015. Micronized copper wood preservatives: an efficiency and potential health risk assessment for copper-based nanoparticles. Environ. Pollut. 200, 126–132.

Cobo, E.R., Kissoon-Singh, V., Moreau, F., Chadee, K., 2015. Colonic MUC2 mucin regulates the expression and antimicrobial activity of β-defensin 2. Mucosal Immunol. 8 (6), 1360–1372.

Cooper, K.L., Liu, K.J., Hudson, L.G., 2009. Enhanced ROS production and redox signaling with combined arsenite and UVA exposure: contribution of NADPH oxidase. Free Radic. Biol. Med. 47 (4), 381–388.

Cornick, S., Tawiah, A., Chadee, K., 2015. Roles and regulation of the mucus barrier in the gut. Tissue Barriers. 3 (1–2), e982426.

Cuillel, M., Chevallet, M., Charbonnier, P., Fauquant, C., Pignot-Paintrand, I., Arnaud, J., Cassio, D., Michaud-Soret, I., Mintz, E., 2014. Interference of CuO nanoparticles with metal homeostasis in hepatocytes under sub-toxic conditions. Nanoscale 6 (3), 1707–1715.

De Jong, W.H., De Rijk, E., Bonetto, A., Wohlleben, W., Stone, V., Brunelli, A., Badetti, E., Marcomini, A., Gosens, I., Cassee, F.R., 2019. Toxicity of copper oxide and basic copper carbonate nanoparticles after short-term oral exposure in rats. Nanotoxicol. 13 (1), 50–72.

Dekkers, S., Williams, T.D., Zhang, J., Zhou, J.A., Vandebriel, R.J., De La Fonteyne, L.J., Gremmer, E.R., He, S., Guggenheim, E.J., Lynch, I., Cassee, F.R., 2018. Multi-omics approaches confirm metal ions mediate the main toxicological pathways of metal-bearing nanoparticles in lung epithelial A549 cells. Environ. Sci. Nano. 5 (6), 1506–1517.

Des Rieux, A., Ragnarsson, E.G., Gullberg, E., Preat, V., Schneider, Y.J., Artursson, P., 2005. Transport of nanoparticles across an *in vitro* model of the human intestinal follicle associated epithelium. Eur. J. Pharm. Sci. 25 (4–5), 455–465.

Domenech, J., Hernández, A., Demir, E., Marcos, R., Cortés, C., 2020a. Interactions of graphene oxide and graphene nanoplatelets with the *in vitro* Caco-2/HT29 model of intestinal barrier. Sci. Rep. 10 (1), 1–15.

Domenech, J., Hernández, A., Rubio, L., Marcos, R., Cortés, C., 2020b. Interactions of polystyrene nanoplastics with *in vitro* models of the human intestinal barrier. Arch. Toxicol. 94 (9), 2997–3012.

Dorier, M., Béal, D., Marie-Desvergne, C., Dubosson, M., Barreau, F., Houdeau, E., Herlin-Boime, N., Carriere, M., 2017. Continuous *in vitro* exposure of intestinal epithelial cells to E171 food additive causes oxidative stress, inducing oxidation of DNA bases but no endoplasmic reticulum stress. Nanotoxicol. 11 (6), 751–761.

Dorier, M., Béal, D., Tisseyre, C., Marie-Desvergne, C., Dubosson, M., Barreau, F., Houdeau, E., Herlin-Boime, N., Rabilloud, T., Carrière, M., 2019. The food additive E171 and titanium dioxide nanoparticles indirectly alter the homeostasis of human intestinal epithelial cells *in vitro*. Environ. Sci. Nano 6 (5), 1549–1561.

Ebabe Elle, R., Rahmani, S., Lauret, C., Morena, M., Bidel, L.P.R., Boulahtouf, A., Balaguer, P., Cristol, J.P., Durand, J.O., Charnay, C., Badia, E., 2016. Functionalized mesoporous silica nanoparticle with antioxidants as a new carrier that generates lower oxidative stress impact on cells. Mol. Pharm. 13 (8), 2647–2660.
Elamin, E., Masclee, A., Troost, F., Dekker, J., Jonkers, D., 2014. Cytotoxicity and metabolic stress induced by acetaldehyde in human intestinal LS174T goblet-like cells. Am. J. Physiol. Gastrointest. Liver Physiol. 307 (3), G286–G294.
Fahmy, B., Cormier, S.A., 2009. Copper oxide nanoparticles induce oxidative stress and cytotoxicity in airway epithelial cells. Toxicol. in Vitro 23 (7), 1365–1371.
Foucaud, L., Wilson, M.R., Brown, D.M., Stone, V., 2007. Measurement of reactive species production by nanoparticles prepared in biologically relevant media. Toxicol. Lett. 174 (1), 1–9.
Fu, P.P., Xia, Q., Hwang, H.M., Ray, P.C., Yu, H., 2014. Mechanisms of nanotoxicity: generation of reactive oxygen species. J. Food Drug Anal. 22 (1), 64–75.
Gabbay, J., 2006. Copper oxide impregnated textiles with potent biocidal activities. J. Ind. Text. 35 (4), 323–335.
Georgantzopoulou, A., Serchi, T., Cambier, S., Leclercq, C.C., Renaut, J., Shao, J., Kruszewski, M., Lentzen, E., Grysan, P., Eswara, S., Audinot, J.N., Contal, S., Ziebel, J., Guignard, C., Hoffmann, L., Murk, A.J., Gutleb, A.C., 2016. Effects of silver nanoparticles and ions on a co-culture model for the gastrointestinal epithelium. Part. Fibre Toxicol. 13 (1), 9.
Gerloff, K., Pereira, D.I.A., Faria, N., Boots, A.W., Kolling, J., Förster, I., Albrecht, C., Powell, J.J., Schins, R.P.F., 2013. Influence of simulated gastrointestinal conditions on particle-induced cytotoxicity and interleukin-8 regulation in differentiated and undifferentiated Caco-2 cells. Nanotoxicol. 7 (4), 353–366.
Gosens, I., Cassee, F.R., Zanella, M., Manodori, L., Brunelli, A., Costa, A.L., Bokkers, B.G. H., de Jong, W.H., Brown, D., Hristozov, D., Stone, V., 2016. Organ burden and pulmonary toxicity of nano-sized copper (II) oxide particles after short-term inhalation exposure. Nanotoxicol. 10 (8), 1084–1095.
Gullberg, E., Leonard, M., Karlsson, J., Hopkins, A.M., Brayden, D., Baird, A.W., Artursson, P., 2000. Expression of specific markers and particle transport in a new human intestinal M-cell model. Biochem. Biophys. Res. Commun. 279 (3), 808–813.
Hansson, G.C., 2012. Role of mucus layers in gut infection and inflammation. Curr. Opin. Microbiol. 15 (1), 57–62.
Hsiao, I.L., Hsieh, Y.K., Wang, C.F., Chen, I.C., Huang, Y.J., 2015. Trojan-horse mechanism in the cellular uptake of silver nanoparticles verified by direct intra- and extracellular silver speciation analysis. Environ. Sci. Technol. 49 (6), 3813–3821.
Huang, Y.W., Wu, C.H., Aronstam, R.S., 2010. Toxicity of transition metal oxide nanoparticles: recent insights from *in vitro* studies. Mater. 3 (10), 4842–4859.
Ivask, A., Juganson, K., Bondarenko, O., Mortimer, M., Aruoja, V., Kasemets, K., Blinova, I., Heinlaan, M., Slaveykova, V., Kahru, A., 2014. Mechanisms of toxic action of Ag, ZnO and CuO nanoparticles to selected ecotoxicological test organisms and mammalian cells *in vitro*: a comparative review. Nanotoxicol. 8 (Sup 1), 57–71.
Jacobsen, N.R., Pojano, G., Wallin, H., Jensen, K.A., 2010. Nanomaterial dispersion protocol for toxicological studies in ENPRA. In: Internal ENPRA Project Report. The National 885 Research Centre for the Working Environment.
Jepson, M.A., Clark, M.A., 2001. The role of M cells in Salmonella infection. Microbes Infect. 3 (14), 1183–1190.
Jiménez, I., Aracena, P., Letelier, M.E., Navarro, P., Speisky, H., 2002. Chronic exposure of HepG2 cells to excess copper results in depletion of glutathione and induction of metallothionein. Toxicol. in Vitro 16 (2), 167–175.
Johnston, H.J., Verdon, R., Gillies, S., Brown, D.M., Fernandes, T.F., Henry, T.B., Rossi, A.G., Tran, L., Tucker, C., Tyler, C.R., Stone, V., 2018. Adoption of *in vitro* systems and zebrafish embryos as alternative models for reducing rodent use in assessments of immunological and oxidative stress responses to nanomaterials. Crit. Rev. Toxicol. 2018 48 (3), 252–271.
Kämpfer, A.A., Busch, M., Schins, R.P., 2020. Advanced *in vitro* testing strategies and models of the intestine for nanosafety research. Chem. Res. Toxicol. 33 (5), 1163–1178.
Karlsson, H.L., Cronholm, P., Gustafsson, J., Möller, L., 2008. Copper oxide nanoparticles are highly toxic: A comparison between metal oxide nanoparticles and carbon nanotubes. Chem. Res. Toxicol. 21 (9), 1726–1732.
Kim, M.J., Lee, H.H., Jeong, J.W., Seo, M.J., Kang, B.W., Park, J.U., Kim, K.S., Cho, Y.S., Seo, K.I., Kim, G.Y., Kim, J.I., Choi, Y.H., Jeong, Y.K., 2014. Anti-inflammatory effects of 5-hydroxy-3,6,7,8,3′,4′-hexamethoxyflavone via NF-kappaB inactivation in lipopolysaccharide-stimulated RAW 264.7 macrophage. Mol. Med. Rep. 9 (4), 1197–1203.
Krüger, K., Cossais, F., Neve, H., Klempt, M., 2014. Titanium dioxide nanoparticles activate IL8-related inflammatory pathways in human colonic epithelial Caco-2 cells. J. Nanopart. Res. 16 (5), 2402.
Kung, M.L., Hsieh, S.L., Wu, C.C., Chu, T.H., Lin, Y.C., Yeh, B.W., Hsieh, S., 2015. Enhanced reactive oxygen species overexpression by CuO nanoparticles in poorly differentiated hepatocellular carcinoma cells. Nanoscale. 7 (5), 1820–1829.
Lee, S.J., Jung, Y.H., Oh, S.Y., Jang, K.K., Lee, H.S., Choi, S.H., Han, H.J., 2015. Vibrio vulnificus VvpE inhibits mucin 2 expression by hypermethylation via lipid raft-mediated ROS signalling in intestinal epithelial cells. Cell Death Dis. 6 (6), e1787.
Lefebvre, D.E., Venema, K., Gombau, L., Valerio Jr., L.G., Raju, J., Bondy, G.S., Bouwmeester, H., Singh, R.P., Clippinger, A.J., Collnot, E.M., Mehta, R., Stone, V., 2015. Utility of models of the gastrointestinal tract for assessment of the digestion and absorption of engineered nanomaterials released from food matrices. Nanotoxicol. 9 (4), 523–542.
Li, J., Song, Y., Vogt, R.D., Liu, Y., Luo, J., Li, T., 2020. Bioavailability and cytotoxicity of cerium-(IV), copper-(II), and zinc oxide nanoparticles to human intestinal and liver cells through food. Sci. Total Environ. 702, 134700.
Lipovsky, A., Tzitrinovich, Z., Friedmann, H., Applerot, G., Gedanken, A., Lubart, R., 2009. EPR study of visible light-induced ROS generation by nanoparticles of ZnO. J. Phys. Chem. C 113 (36), 15997–16001.
Liu, S., Kawai, K., Tyurin, V.A., Tyurina, Y.Y., Borisenko, G.G., Fabisiak, J.P., Quinn, P.J., Pitt, B.R., Kagan, V.E., 2001. Nitric oxide-dependent pro-oxidant and pro-apoptotic effect of metallothioneins in HL-60 cells challenged with cupric nitrilotriacetate. Biochem. J. 354 (Pt 2), 397–406.
Long, T.C., Saleh, N., Tilton, R.D., Lowry, G.V., Veronesi, B., 2006. Titanium dioxide (P25) produces reactive oxygen species in immortalized brain microglia (BV2): implications for nanoparticle neurotoxicity. Environ. Sci. Technol. 40 (14), 4346–4352.
Luther, E.M., Schmidt, M.M., Diendorf, J., Epple, M., Dringen, R., 2012. Upregulation of metallothioneins after exposure of cultured primary astrocytes to silver nanoparticles. Neurochem. Res. 37 (8), 1639–1648.
Mahler, G.J., Shuler, M.L., Glahn, R.P., 2009. Characterization of Caco-2 and HT29-MTX cocultures in an *in vitro* digestion/cell culture model used to predict iron bioavailability. J. Nutr. Biochem. 20 (7), 494–502.
Marano, F., Hussain, S., Rodrigues-Lima, F., Baeza-Squiban, A., Boland, S., 2011. Nanoparticles: molecular targets and cell signalling. Arch. Toxicol. 85 (7), 733–741.
Mercier-Bonin, M., Despax, B., Raynaud, P., Houdeau, E., Thomas, M., 2018. Mucus and microbiota as emerging players in gut nanotoxicology: the example of dietary silver and titanium dioxide nanoparticles. Crit. Rev. Food Sci. Nutr. 58 (6), 1023–1032.
Miura, N., Shinohara, Y., 2009. Cytotoxic effect and apoptosis induction by silver nanoparticles in HeLa cells. Biochem. Biophys. Res. Commun. 390 (3), 733–737.
Pavelić, K., Hadžija, M., Bedrica, L., Pavelić, J., Đikić, I., Katić, M., Kralj, M., Bosnar, M. H., Kapitanović, S., Poljak-Blaži, M., Križanac, Š., 2001. Natural zeolite clinoptilolite: new adjuvant in anticancer therapy. J. Mol. Med. 78 (12), 708–720.
Peijnenburg, W.J., Ruggiero, E., Boyles, M., Murphy, F., Stone, V., Elam, D.A., Werle, K., Wohlleben, W., 2020. A method to assess the relevance of nanomaterial dissolution during reactivity testing. Materials 13 (10), 2235.
Piana, C., Wirth, M., Gerbes, S., Viernstein, H., Gabor, F., Toegel, S., 2008. Validation of reference genes for qPCR studies on Caco-2 cell differentiation. Eur. J. Pharm. Biopharm. 69 (3), 1187–1192.
Piret, J.P., Jacques, D., Audinot, J.N., Mejia, J., Boilan, E., Noël, F., Fransolet, M., Demazy, C., Lucas, S., Saout, C., Toussaint, O., 2012a. Copper (II) oxide nanoparticles penetrate into HepG2 cells, exert cytotoxicity via oxidative stress and induce pro-inflammatory response. Nanoscale 4 (22), 7168–7184.
Piret, J.P., Vankoningsloo, S., Mejia, J., Noel, F., Boilan, E., Lambinon, F., Zouboulis, C. C., Masereel, B., Lucas, S., Saout, C., Toussaint, O., 2012b. Differential toxicity of copper (II) oxide nanoparticles of similar hydrodynamic diameter on human differentiated intestinal Caco-2 cell monolayers is correlated in part to copper release and shape. Nanotoxicol. 6 (7), 789–803.
Ruttkay-Nedecky, B., Nejdl, L., Gumulec, J., Zitka, O., Masarik, M., Eckschlager, T., Stiborova, M., Adam, V., Kizek, R., 2013. The role of metallothionein in oxidative stress. Int. J. Mol. Sci. 14 (3), 6044–6066.
Ryu, W.I., Park, Y.H., Bae, H.C., Kim, J.H., Jeong, S.H., Lee, H., Son, S.W., 2014. ZnO nanoparticle induces apoptosis by ROS triggered mitochondrial pathway in human keratinocytes. Mol. Cell. Toxicol. 10 (4), 387–391.
Sabella, S., Carney, R.P., Brunetti, V., Malvindi, M.A., Al-Juffali, N., Vecchio, G., Janes, S. M., Bakr, O.M., Cingolani, R., Stellacci, F., 2014. A general mechanism for intracellular toxicity of metal-containing nanoparticles. Nanoscale. 6 (12), 7052–7061.
Sahu, D., Kannan, G.M., Vijayaraghavan, R., Anand, T., Khanum, F., 2013. Nanosized zinc oxide induces toxicity in human lung cells. ISRN Toxicol. 2013.
Sambuy, Y., Ferruzza, S., Ranaldi, G., De Angelis, I., 2001. Intestinal cell culture models: applications in toxicology and pharmacology. Cell Biol. Toxicol. 17, 301–311.
Sambuy, Y., De Angelis, I., Ranaldi, G., Scarino, M.L., Stammati, A., Zucco, F., 2005. The Caco-2 cell line as a model of the intestinal barrier: influence of cell and culture-related factors on Caco-2 cell functional characteristics. Cell Biol. Toxicol. 21, 1–26.
Sauvain, J.J., Rossi, M.J., Riediker, M., 2013. Comparison of three acellular tests for assessing the oxidation potential of nanomaterials. Aerosol Sci. Technol. 47 (2), 218–227.
Schimpel, C., Teubl, B., Absenger, M., Meindl, C., Fröhlich, E., Leitinger, G., Zimmer, A., Roblegg, E., 2014. Development of an advanced intestinal *in vitro* triple culture permeability model to study transport of nanoparticles. Mol. Pharm. 11 (3), 808–818.
Shinohara, N., Zhang, G., Oshima, Y., Kobayashi, T., Imatanaka, N., Nakai, M., Sasaki, T., Kawaguchi, K., Gamo, M., 2017. Kinetics and dissolution of intratracheally administered nickel oxide nanomaterials in rats. Part. Fibre Toxicol. 14, 48.
Song, Y., Guan, R., Lyu, F., Kang, T., Wu, Y., Chen, X., 2014. *In vitro* cytotoxicity of silver nanoparticles and zinc oxide nanoparticles to human epithelial colorectal adenocarcinoma (Caco-2) cells. Mutat. Res. Fundam. Mol. Mech. Mutagen. 769, 113–118.
Sthijns, M.M.J.P.E., Thongkam, W., Albrecht, C., Hellack, B., Bast, A., Haenen, G.R.M.M., Schins, R.P.F., 2017. Silver nanoparticles induce hormesis in A549 human epithelial cells. Toxicol. in Vitro 40, 223–233.
Stone, V., Brown, D.M., Watt, N., Wilson, M., Donaldson, K., Ritchie, H., MacNee, W., 2000. Ultrafine particle-mediated activation of macrophages: intracellular calcium signaling and oxidative stress. Inhal. Toxicol. 12 (3), 345–351.
Stone, V., Miller, M.R., Clift, M.J., Elder, A., Mills, N.L., Møller, P., Schins, R.P., Vogel, U., Kreyling, W.G., Alstrup Jensen, K., Kuhlbusch, T.A., 2017. Nanomaterials versus ambient ultrafine particles: an opportunity to exchange toxicology knowledge. Environ. Health Perspect. 125 (10), 106002–106017.
Strauch, B.M., Niemand, R.K., Winkelbeiner, N.L., Hartwig, A., 2017. Comparison between micro- and nanosized copper oxide and water-soluble copper chloride:

interrelationship between intracellular copper concentrations, oxidative stress and DNA damage response in human lung cells. Part. Fibre Toxicol. 14, 28.
Struyf, S., Gouwy, M., Dillen, C., Proost, P., Opdenakker, G., Van Damme, J., 2005. Chemokines synergize in the recruitment of circulating neutrophils into inflamed tissue. Eur. J. Immunol. 35 (5), 1583–1591.
Suzuki, K.T., Someya, A., Komada, Y., Ogra, Y., 2002. Roles of metallothionein in copper homeostasis: responses to Cu-deficient diets in mice. J. Inorg. Biochem. 88, 173–182.
Tada-Oikawa, S., Ichihara, G., Fukatsu, H., Shimanuki, Y., Tanaka, N., Watanabe, E., Suzuki, Y., Murakami, M., Izuoka, K., Chang, J., Wu, W., 2016. Titanium dioxide particle type and concentration influence the inflammatory response in Caco-2 cells. Int. J. Mol. Sci. 17 (4), 576.
Tadesse, S., Corner, G., Dhima, E., Houston, M., Guha, C., Augenlicht, L., Velcich, A., 2017. MUC2 mucin deficiency alters inflammatory and metabolic pathways in the mouse intestinal mucosa. Oncotarget. 8 (42), 71456–71470.
Tailford, L.E., Crost, E.H., Kavanaugh, D., Juge, N., 2015. Mucin glycan foraging in the human gut microbiome. Front. Genet. 6, 81.
Takahashi, S., 2012. Molecular functions of metallothionein and its role in hematological malignancies. J. Hematol. Oncol. 5, 41.
Triboulet, S., Aude-Garcia, C., Armand, L., Collin-Faure, V., Chevallet, M., Diemer, H., Gerdil, A., Proamer, F., Strub, J.M., Habert, A., Herlin, N., 2015. Comparative proteomic analysis of the molecular responses of mouse macrophages to titanium dioxide and copper oxide nanoparticles unravels some toxic mechanisms for copper oxide nanoparticles in macrophages. PLoS One 10 (4), e0124496.
Tsuji, T., Kato, A., Yasuda, H., Miyaji, T., Luo, J., Sakao, Y., Ito, H., Fujigaki, Y., Hishida, A., 2009. The dimethylthiourea-induced attenuation of cisplatin nephrotoxicity is associated with the augmented induction of heat shock proteins. Toxicol. Appl. Pharmacol. 234 (2), 202–208.
Ude, V.C., Brown, D.M., Viale, L., Kanase, N., Stone, V., Johnston, H.J., 2017. Impact of copper oxide nanomaterials on differentiated and undifferentiated Caco-2 intestinal epithelial cells; assessment of cytotoxicity, barrier integrity, cytokine production and nanomaterial penetration. Part. Fibre Toxicol 14 (1), 31.
Ude, V.C., Brown, D.M., Stone, V., Johnston, H.J., 2019a. Using 3D gastrointestinal tract *in vitro* models with microfold cells and mucus secreting ability to assess the hazard of copper oxide nanomaterials. J. Nanobiotechnol. 17 (1), 70.
Ude, V.C., Brown, D.M., Maciaszek, K., Stone, V., Johnston, H.J., 2019b. The sensitivity of different intestinal Caco-2 *in vitro* monocultures and co-cultures to amorphous silicon dioxide nanomaterials and the clay montmorillonite. NanoImpact 15, 100165.
Valko, M., Leibfritz, D., Moncol, J., Cronin, M.T., Mazur, M., Telser, J., 2007. Free radicals and antioxidants in normal physiological functions and human disease. Int. J. Biochem. Cell Biol. 39 (1), 44–84.
Vreeburg, R.A.M., Bastiaan-Net, S., Mes, J.J., 2011. Normalization genes for quantitative RT-PCR in differentiated Caco-2 cells used for food exposure studies. Food Funct. 2 (2), 124–129.
Wang, Z., Li, N., Zhao, J., White, J.C., Qu, P., Xing, B., 2012. CuO nanoparticle interaction with human epithelial cells: cellular uptake, location, export, and genotoxicity. Chem. Res. Toxicol. 25 (7), 1512–1521.
Yan, H., Duan, X., Pan, H., Holguin, N., Rai, M.F., Akk, A., Springer, L.E., Wickline, S.A., Sandell, L.J., Pham, C.T.N., 2016. Suppression of NF-κB activity via nanoparticle-based siRNA delivery alters early cartilage responses to injury. Proc. Natl. Acad. Sci. U. S. A. 113 (41), E6199–E6208.
Yan, Z., Wang, W., Wu, Y., Wang, W., Li, B., Liang, N., Wu, W., 2017. Zinc oxide nanoparticle-induced atherosclerotic alterations *in vitro* and *in vivo*. Int. J. Nanomedicine 2017, 4433–4442 [Online].
Zhang, H., Wang, X., Wang, M., Li, L., Chang, C.H., Ji, Z., Xia, T., Nel, A.E., 2015. Mammalian cells exhibit a range of sensitivities to silver nanoparticles that are partially explicable by variations in antioxidant defence and metallothionein expression. Small. 11 (31), 3797–3805.
Zhang, X.F., Shen, W., Gurunathan, S., 2016. Silver nanoparticle-mediated cellular responses in various cell lines: an *in vitro* model. Int. J. Mol. Sci. 17 (10), 1603.
Zhao, Z., Qu, W., Wang, K., Chen, S., Zhang, L., Wu, D., Chen, Z., 2019. Bisphenol A inhibits mucin 2 secretion in intestinal goblet cells through mitochondrial dysfunction and oxidative stress. Biomed. Pharmacother. 111, 901–908.
Zhu, X., Fan, W.G., Li, D.P., Kung, H., Lin, M.C., 2011. Heme oxygenase-1 system and gastrointestinal inflammation: a short review. World J. Gastroenterol. 17 (38), 4283–4288.